

Machine learning dismantling and early-warning signals of disintegration in complex systems

Marco Grassia¹, Manlio De Domenico^{2*}, Giuseppe Mangioni^{1*}

¹Dip. Ingegneria Elettrica, Elettronica e Informatica - Università degli Studi di Catania - Italy

²CoMuNe Lab, Fondazione Bruno Kessler, Via Sommarive 18, 38123 Povo (TN), Italy

*To whom correspondence should be addressed;

E-mail: giuseppe.mangioni@dieei.unict.it; mdedomenico@fbk.eu.

From physics to engineering, biology and social science, natural and artificial systems are characterized by interconnected topologies whose features – e.g., heterogeneous connectivity, mesoscale organization, hierarchy – affect their robustness to external perturbations, such as targeted attacks to their units. Identifying the minimal set of units to attack to disintegrate a complex network, i.e. network dismantling, is a computationally challenging (NP-hard) problem which is usually attacked with heuristics. Here, we show that a machine trained to dismantle relatively small systems is able to identify higher-order topological patterns, allowing to disintegrate large-scale social, infrastructural and technological networks more efficiently than human-based heuristics. Remarkably, the machine assesses the probability that next attacks will disintegrate the system, providing a quantitative method to quantify systemic risk and detect early-warning signals of system’s collapse. This demonstrates that machine-assisted analysis can be effectively used for policy and

decision making to better quantify the fragility of complex systems and their response to shocks.

Introduction

Several empirical systems consist of nonlinearly interacting units, whose structure and dynamics can be suitably represented by complex networks (11). Heterogeneous connectivity (4), mesoscale (19, 31), higher-order (9, 26) and hierarchical (15) organization, efficiency in information exchange (43) and multiplexity (10, 17, 18, 25), are distinctive features of biological molecules within the cell (20), connectomes (8), mutualistic interactions among species (39), urban (6), trade (2) and social (14, 22, 27) systems.

However, the structure of complex networks can dramatically affect its proper functioning, with crucial effects on collective behavior and phenomena such as synchronization in populations of coupled oscillators (3), the spreading of infectious diseases (28, 33) and cascade failures (44), the emergence of misinformation (38, 42) and hate (23) in socio-technical systems or the emergence of social conventions (5). While heterogeneous connectivity is known to make such complex networks more sensitive to shocks and other perturbations occurring to hubs (1), a clear understanding of the topological factors – and their interplay – responsible for a system’s vulnerability still remains elusive. For this reason, the identification of the minimum set of units to target for driving a system towards its collapse – a procedure known as network dismantling – attracted increasing attention (12, 24, 29, 30, 36) for practical applications and their implications for policy making. Dismantling is efficient if such a set is small and, simultaneously, the system quickly breaks down into smaller isolated clusters. The problem is, however, NP-hard and while percolation theory provides the tools to understand large-scale transitions as units are randomly disconnected (7, 13, 32, 35), a general theory of network dismantling is missing and applications mostly rely on approximated theories or heuristics.

Here, we develop a computationally efficient framework – named GDM and conceptually described in Figure 1 – based on machine learning, to provide a scalable solution, tackle the dismantling challenge, and gain new insights about the latent features of the topological organization of complex networks. Specifically, we employ graph convolutional-style layers, overcoming the limitations of classic (Euclidean) deep learning and operate on graph-structured data. These layers, inspired by the convolutional layers that empower most of the deep learning models nowadays, aggregate the features of each node with the ones found in its neighborhood by means of a learned non-trivial function, producing high-level node features. While the machine is trained on identifying the critical point from dismantling of relatively small systems – that can be easily and optimally dismantled – we show that it exhibits remarkable inductive capabilities, being able to generalize to previously unseen nodes and way larger networks after the learning phase.

Results

Model architecture

The machine learning framework proposed here consists of a (geometric) deep learning model, composed of graph convolutional-style layers and a regressor (a multilayer perceptron), that is trained to predict attack strategies on small synthetic networks – that can be easily and optimally dismantled – and then used to dismantle large networks, for which the optimal solution cannot be found in reasonable time. To give an insight, the graph convolutional-style layers aggregate the features of each node with the ones found in its neighborhood by means of a learned non-trivial function, as they are inspired by the convolutional layers that empower most of the (Euclidean) deep learning models nowadays. More practically, the (higher-order) node features are propagated by the neural network when many layers are stacked: deeper the architecture, i.e., the more convolutional layers, the farther the features propagate, capturing

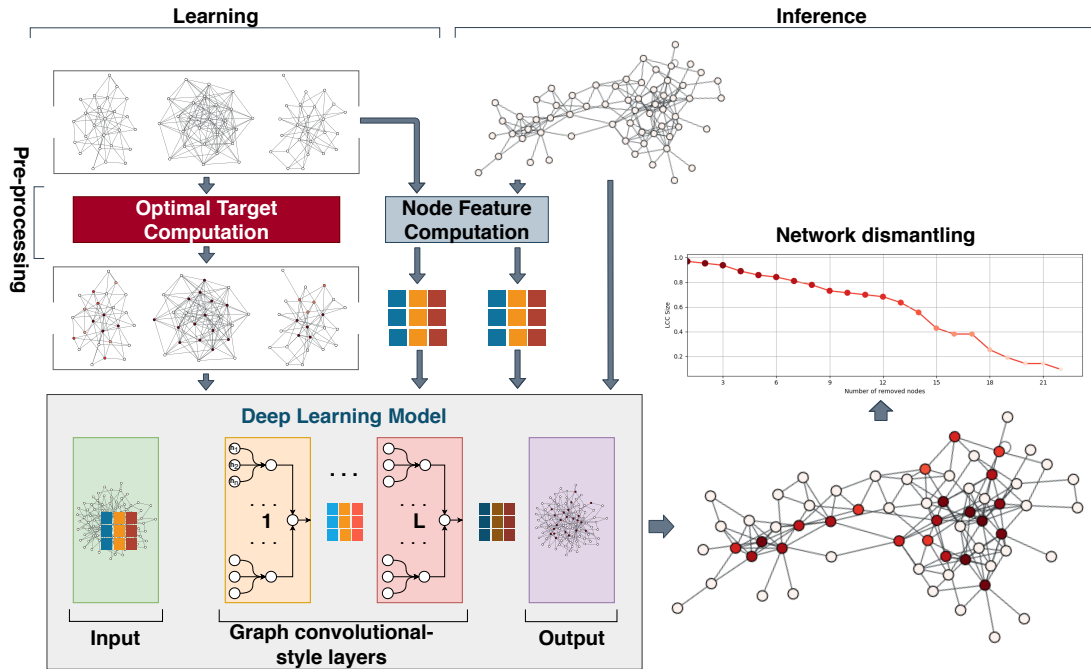


Figure 1: **Training a machine to learn complex topological patterns for network dismantling.** To build our training data, we generate and dismantle small networks optimally and compute the node features. After the model is trained, it can be fed the target network (again, with its nodes' features) and it will assign each node n a value p_n , the probability that it belongs to the (sub-)optimal dismantling set. Nodes are then ranked and removed until the dismantling target is reached.

the importance of the neighborhood of each node. Specifically, we stack a variable number of state-of-the-art layers, namely *Graph Attention Networks (GAT)* (41), that are based on the self-attention mechanism (also known as intra-attention) which was shown to improve the performance in natural language processing tasks (40). These layers are able to handle the whole neighborhood of nodes without any sampling, which is one of the major limitations of other popular convolutional-style layers (e.g., *GraphSage* (21)), and also to assign a relative importance factor to the features of each neighboring node that depends on the node itself thanks to the attention mechanism.

Such detailed model takes as input one network at a time plus the features of its nodes and returns a scalar value p_n between zero and one for every node n . During the dismantling of a network, nodes are sorted and removed (if they belong to the LCC) in descending order of p_n until the target is reached.

Dismantling real-world systems

In our experiments, we dismantle empirical complex systems of high societal or strategic relevance, our main goal being to learn an efficient attack strategy. To validate the goodness of such a strategy, we compare against state-of-the-art dismantling methods, such as *Generalized Network Dismantling (GND)* (36), *Explosive Immunization (EI)* (16), *CoreHD* (45), *Min-Sum (MS)* (12) and *Collective Influence (CI)* (30), using node degree, k -core value and local clustering coefficient as node features.

We refer the reader to the Supplementary Materials for a detailed description of our models, for additional discussion and experiments (also on large real-world and synthetic networks, plus results in table form), and also for an extensive list of the real-world test networks, that include biological, social, infrastructure, communication, trophic and technological ones.

To quantify the goodness of each method in dismantling the network, we consider the *Area*

Under the Curve (AUC) encoding changes in the *Largest Connected Component* (LCC) size across the attacks. The LCC size is commonly used in the literature to quantify the robustness of a network, because systems need the existence of a giant cluster to work properly. The AUC indicator¹ has the advantage of accounting for how quickly, overall, the LCC is disintegrated: the lower the area under the curve, the more efficient is the network dismantling.

As a representative example, we show in Figure 2a the result of the dismantling process for the *corruption* network (37), built from 65 corruption scandals in Brazil, as a function of the number of removed units. Results are shown for GDM and the two cutting-edge algorithms mentioned above. In Figures 2b and 2c, instead, we show the structure before and after dismantling, respectively. Our framework disintegrates the network faster than other methods: to verify if this feature is general, we perform a thorough analysis of several empirical systems.

Figure 3 shows the performance of each dismantling method on each empirical system considered in this study, allowing for an overall comparison. On average, our approach outperforms the others. For instance, Generalized Network Dismantling’s cumulative AUC is $\sim 12\%$ higher and the Min-Sum algorithm is outscored by a significant margin, which is remarkable considering that our approach is static – i.e., predictions are made at the beginning of the attack – while the other ones are dynamic – i.e., structural importance of the nodes is (re)computed during the attacks. For a more extensive comparison with these approaches, we also introduce a node reinsertion phase using a greedy algorithm which reinserts, a posteriori, those nodes that belong to smaller components of the (virtually) dismantled system and which removal is not actually needed in order to reach the desired target (12). Once again, our approach outperforms the other algorithms: even without accounting for the reinsertion phase, GDM performs comparably with GND + reinsertion and outscores the others, highlighting how it is able to identify the more critical nodes of a network.

¹We compute the AUC value by integrating the $LCC(x)/|N|$ values using Simpson’s rule.

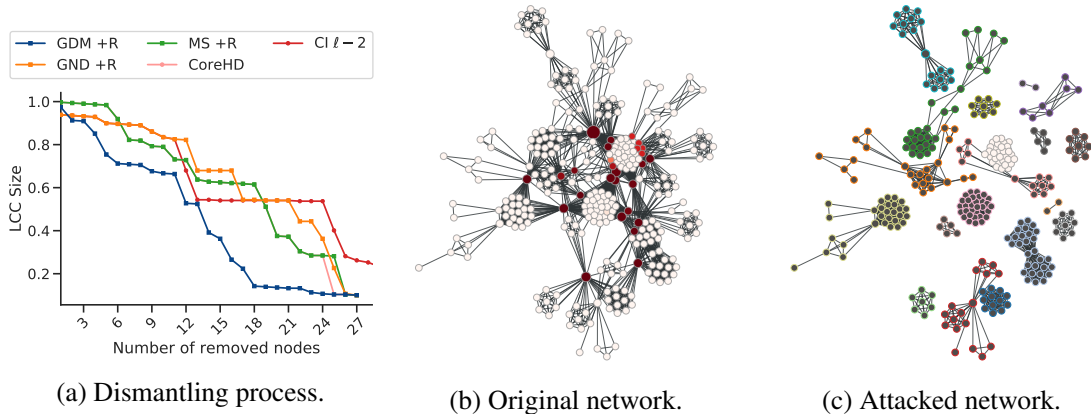


Figure 2: Dismantling the Brazilian corruption network. (a) GDM and state-of-the-art algorithms with reinsertion of the nodes are compared. The network before (b) and after (c) a GDM attack is shown. The color of the nodes represents (from dark red to white) the attack order, while their size represents their betweenness value. In the attacked network, darker nodes do not belong to the LCC, and their contour color represents the component they belong to.

An interesting feature of our framework is that it can enhance existing heuristics based on node descriptors, by employing the same measure as the only node feature. It is plausible to assess that our framework learns correlations among node features. To probe this hypothesis, in the Supplementary Materials we analyze the configuration models of the same networks analyzed so far: those models keep the observed connectivity distribution while destroying topological correlations. We observe that dismantling performance drop on these models, confirming that the existing topological correlations are learned and, consequently, exploited by the machine.

Early-warning signals of systemic collapse

Another relevant output of our method is the calculation of a damage score that can be used to predict the impact of future attacks to the system. Accordingly, we introduce an estimator of early warning that can be used for inform policy and decision making in applications where complex interconnected systems – such as water management systems, power grids, communi-

cation systems and public transportation networks – are subject to potential failures or targeted attacks. We define Ω , namely *Early Warning*, as a value between 0 and 1, calculated as follows. We first simulate the dismantling of the target network using our approach and call S_o the set of virtually removed nodes that cause the percolation of the network. Then, we sum the p_n values predicted by our model for each node $n \in S_o$ and define

$$\Omega_m = \sum_{n \in S_o} p_n.$$

The value of the Early Warning Ω for the network after the removal of a generic set S of nodes is given by

$$\Omega = \begin{cases} \Omega_s / \Omega_m & \text{if } \Omega_s \leq \Omega_m \\ 1 & \text{otherwise} \end{cases}$$

where $\Omega_s = \sum_{n \in S} p_n$.

The rationale behind this definition is that the system will tolerate a certain amount of damage before it collapses: this value is captured by Ω_m . Ω will quickly reach values close to 1 when nodes with key-role in the integrity of the system are removed. Of course, the system could be heavily harmed by removing many less relevant nodes (e.g., the peripheral ones) with an attack that causes a small decrease in LCC size over time, and probably get a low value of Ω . However, this kind of attacks does not need an early-warning signal since they do not cause an abrupt disruption of the system and can be easily detected.

Why do we need an Early Warning signal? In Figure 4 we show a toy-example meant to explain why the Largest Connected Component size may not be enough to determine the state of a system. The toy-example network in Figure 4a is composed of two cliques (fully connected sub-networks) connected by a few border nodes (bridges) that also belong to the respective cliques. Many dismantling approaches (like the degree and betweenness-based heuristics, or even ours) would remove those bridge nodes first, meaning that the network would eventually

break in two, as shown in Figure 4b. Now, when most of the bridge nodes are removed (e.g., after 16 removals), the LCC is still quite large as it includes more than 80% of the nodes, but it takes just a few more removals of the bridges to break the network in two. While Ω is able to capture the imminent system disruption (i.e., the Ω value gets closer to 1 very fast), the LCC size is not, and one would notice when it is too late. Moreover, the LCC curve during the initial part of the attack is exactly the same as the one in Figure 4c, showing the removal of nodes in inverse degree (or betweenness) order, which does not cause the percolation of the system. Again, Ω captures this difference and does not grow, meaning that a slow degradation should be expected.

Tests on real-world systems We test our method on key infrastructure networks and predict the collapse of the system under various attack strategies (see Fig. 5 for details). Remarkably, while the LCC size decreases slowly without providing a clear alarm signal until the system is heavily damaged and collapses, Ω grows faster when critical nodes are successfully attacked, reaching warning levels way before the system is disrupted, as highlighted by the First Response Time, defined as the time occurring between system’s collapse and an early-warning signal of 50% (i.e., $\Omega = 0.5$). Moreover, the first order derivative Ω'_s tracks the importance of nodes that are being attacked, providing a measure of the attack intensity over time.

Discussion

Our results show that using machine learning to learn network dismantling comes with a series of advantages. While the ultimate theoretical framework is still missing, our framework allows one to learn directly from the data, at variance with traditional approaches which rely on the definition of new heuristics, metrics or algorithms. An important advantage of our method, typical of data-driven modeling, is that it can be further improved by simply retuning the pa-

rameters of the underlying model and training again: conversely, existing approaches require the (re)definition of heuristics and algorithms which are more demanding in terms of human efforts. Remarkably, the computational complexity of dismantling networks with our framework is considerably low: just $O(N + E)$, where N is system's size and E the number of connections – which drops to $O(N)$ for sparse networks. This feature allows for applications to systems consisting of millions of nodes while keeping excellent performance in terms of computing time and accuracy. Last but not least, from a methodological perspective, it is worth remarking that our framework is general enough to be adapted and applied to other interesting NP-hard problems on networks, opening the door for new opportunities and promising research directions in complexity science, together with very recent results employing machine learning, for instance, to predict extreme events (34).

The impact of our results is broad. On the one hand, we provide a framework which disintegrates real systems more efficiently and faster than state-of-the-art approaches: for instance, applications to covert networks might allow to hinder communications and information exchange between harmful individuals. On the other hand, we provide a quantitative descriptor of damage which is more predictive than existing ones, such as the size of the largest connected component: our measure allows to estimate the potential system's collapse due to subsequent damages, providing policy and decision makers with a quantitative early-warning signal for triggering a timely response to systemic emergencies in water management systems, power grids, communication and public transportation networks.

References

1. Réka Albert, Hawoong Jeong, and Albert-László Barabási. Error and attack tolerance of complex networks. *nature*, 406(6794):378, 2000.

2. Luiz G. A. Alves, Giuseppe Mangioni, Isabella Cingolani, Francisco Aparecido Rodrigues, Pietro Panzarasa, and Yamir Moreno. The nested structural organization of the worldwide trade multi-layer network. *Scientific Reports*, 9(1):2866, 2019.
3. Alex Arenas, Albert Díaz-Guilera, Jurgen Kurths, Yamir Moreno, and Changsong Zhou. Synchronization in complex networks. *Physics reports*, 469(3):93–153, 2008.
4. Albert-László Barabási and Réka Albert. Emergence of scaling in random networks. *science*, 286(5439):509–512, 1999.
5. Andrea Baronchelli. The emergence of consensus: a primer. *Royal Society open science*, 5(2):172189, 2018.
6. Marc Barthelemy. The statistical physics of cities. *Nature Reviews Physics*, 1:406–415, 2019.
7. Amir Bashan, Yehiel Berezin, Sergey V Buldyrev, and Shlomo Havlin. The extreme vulnerability of interdependent spatially embedded networks. *Nature Physics*, 9(10):667, 2013.
8. Danielle S Bassett and Olaf Sporns. Network neuroscience. *Nature neuroscience*, 20(3):353, 2017.
9. Austin R Benson, David F Gleich, and Jure Leskovec. Higher-order organization of complex networks. *Science*, 353(6295):163–166, 2016.
10. Stefano Boccaletti, Ginestra Bianconi, Regino Criado, Charo I Del Genio, Jesús Gómez-Gardenes, Miguel Romance, Irene Sendina-Nadal, Zhen Wang, and Massimiliano Zanin. The structure and dynamics of multilayer networks. *Physics Reports*, 544(1):1–122, 2014.
11. Stefano Boccaletti, Vito Latora, Yamir Moreno, Martin Chavez, and D-U Hwang. Complex networks: Structure and dynamics. *Physics reports*, 424(4-5):175–308, 2006.

12. Alfredo Braunstein, Luca Dall'Asta, Guilhem Semerjian, and Lenka Zdeborová. Network dismantling. *Proceedings of the National Academy of Sciences*, 113(44):12368–12373, Oct 2016.
13. Sergey V Buldyrev, Roni Parshani, Gerald Paul, H Eugene Stanley, and Shlomo Havlin. Catastrophic cascade of failures in interdependent networks. *Nature*, 464(7291):1025, 2010.
14. Damon Centola, Joshua Becker, Devon Brackbill, and Andrea Baronchelli. Experimental evidence for tipping points in social convention. *Science*, 360(6393):1116–1119, 2018.
15. Aaron Clauset, Cristopher Moore, and Mark EJ Newman. Hierarchical structure and the prediction of missing links in networks. *Nature*, 453(7191):98, 2008.
16. Pau Clusella, Peter Grassberger, Francisco J. Pérez-Reche, and Antonio Politi. Immunization and targeted destruction of networks using explosive percolation. *Phys. Rev. Lett.*, 117:208301, Nov 2016.
17. Manlio De Domenico, Clara Granell, Mason A Porter, and Alex Arenas. The physics of spreading processes in multilayer networks. *Nature Physics*, 12(10):901–906, 2016.
18. Manlio De Domenico, Albert Solé-Ribalta, Emanuele Cozzo, Mikko Kivelä, Yamir Moreno, Mason A Porter, Sergio Gómez, and Alex Arenas. Mathematical formulation of multilayer networks. *Physical Review X*, 3(4):041022, 2013.
19. Santo Fortunato. Community detection in graphs. *Physics reports*, 486(3-5):75–174, 2010.
20. Roger Guimera and Luis A Nunes Amaral. Functional cartography of complex metabolic networks. *nature*, 433(7028):895, 2005.

21. William L. Hamilton, Rex Ying, and Jure Leskovec. Inductive representation learning on large graphs. 2017.
22. Neil F Johnson, M Zheng, Yulia Vorobyeva, Andrew Gabriel, Hong Qi, Nicolás Velásquez, Pedro Manrique, Daniela Johnson, E Restrepo, Chaoming Song, et al. New online ecology of adversarial aggregates: Isis and beyond. *Science*, 352(6292):1459–1463, 2016.
23. NF Johnson, R Leahy, N Johnson Restrepo, N Velasquez, M Zheng, P Manrique, P Devkota, and S Wuchty. Hidden resilience and adaptive dynamics of the global online hate ecology. *Nature*, 573(7773):261–265, 2019.
24. Maksim Kitsak, Lazaros K Gallos, Shlomo Havlin, Fredrik Liljeros, Lev Muchnik, H Eugene Stanley, and Hernán A Makse. Identification of influential spreaders in complex networks. *Nature physics*, 6(11):888, 2010.
25. Mikko Kivelä, Alex Arenas, Marc Barthelemy, James P Gleeson, Yamir Moreno, and Mason A Porter. Multilayer networks. *Journal of complex networks*, 2(3):203–271, 2014.
26. Renaud Lambiotte, Martin Rosvall, and Ingo Scholtes. From networks to optimal higher-order models of complex systems. *Nature Physics*, 15(4):313–320, 2019.
27. David Lazer, Alex Pentland, Lada Adamic, Sinan Aral, Albert-László Barabási, Devon Brewer, Nicholas Christakis, Noshir Contractor, James Fowler, Myron Gutmann, et al. Computational social science. *Science*, 323(5915):721–723, 2009.
28. Joan T Matamalas, Alex Arenas, and Sergio Gómez. Effective approach to epidemic containment using link equations in complex networks. *Science advances*, 4(12):eaau4212, 2018.

29. Flaviano Morone and Hernán A Makse. Influence maximization in complex networks through optimal percolation. *Nature*, 524(7563):65, 2015.
30. Flaviano Morone, Byungjoon Min, Lin Bo, Romain Mari, and Hernán A Makse. Collective influence algorithm to find influencers via optimal percolation in massively large social media. *Scientific reports*, 6:30062, 2016.
31. Mark EJ Newman. Communities, modules and large-scale structure in networks. *Nature physics*, 8(1):25–31, 2012.
32. Saeed Osat, Ali Faqeeh, and Filippo Radicchi. Optimal percolation on multiplex networks. *Nature communications*, 8(1):1540, 2017.
33. Romualdo Pastor-Satorras, Claudio Castellano, Piet Van Mieghem, and Alessandro Vespignani. Epidemic processes in complex networks. *Reviews of modern physics*, 87(3):925, 2015.
34. Di Qi and Andrew J Majda. Using machine learning to predict extreme events in complex systems. *PNAS*, 117(1):52–59, 2020.
35. Filippo Radicchi. Percolation in real interdependent networks. *Nature Physics*, 11(7):597, 2015.
36. Xiao-Long Ren, Niels Gleinig, Dirk Helbing, and Nino Antulov-Fantulin. Generalized network dismantling. *Proceedings of the National Academy of Sciences*, 116(14):6554–6559, 2019.
37. Haroldo V Ribeiro, Luiz G A Alves, Alvaro F Martins, Ervin K Lenzi, and Matjaž Perc. The dynamical structure of political corruption networks. *Journal of Complex Networks*, 6(6):989–1003, 01 2018.

38. Massimo Stella, Emilio Ferrara, and Manlio De Domenico. Bots increase exposure to negative and inflammatory content in online social systems. *Proceedings of the National Academy of Sciences*, 115(49):12435–12440, 2018.
39. Samir Suweis, Filippo Simini, Jayanth R Banavar, and Amos Maritan. Emergence of structural and dynamical properties of ecological mutualistic networks. *Nature*, 500(7463):449, 2013.
40. Ashish Vaswani, Noam Shazeer, Niki Parmar, Jakob Uszkoreit, Llion Jones, Aidan N. Gomez, Lukasz Kaiser, and Illia Polosukhin. Attention is all you need. 06 2017.
41. Petar Veličković, Guillem Cucurull, Arantxa Casanova, Adriana Romero, Pietro Liò, and Yoshua Bengio. Graph attention networks. 2018.
42. Soroush Vosoughi, Deb Roy, and Sinan Aral. The spread of true and false news online. *Science*, 359(6380):1146–1151, 2018.
43. Duncan J Watts and Steven H Strogatz. Collective dynamics of ‘small-world’ networks. *nature*, 393(6684):440, 1998.
44. Yang Yang, Takashi Nishikawa, and Adilson E Motter. Small vulnerable sets determine large network cascades in power grids. *Science*, 358(6365):eaan3184, 2017.
45. Lenka Zdeborová, Pan Zhang, and Hai-Jun Zhou. Fast and simple decycling and dismantling of networks. *Scientific Reports*, 6(1), Nov 2016.

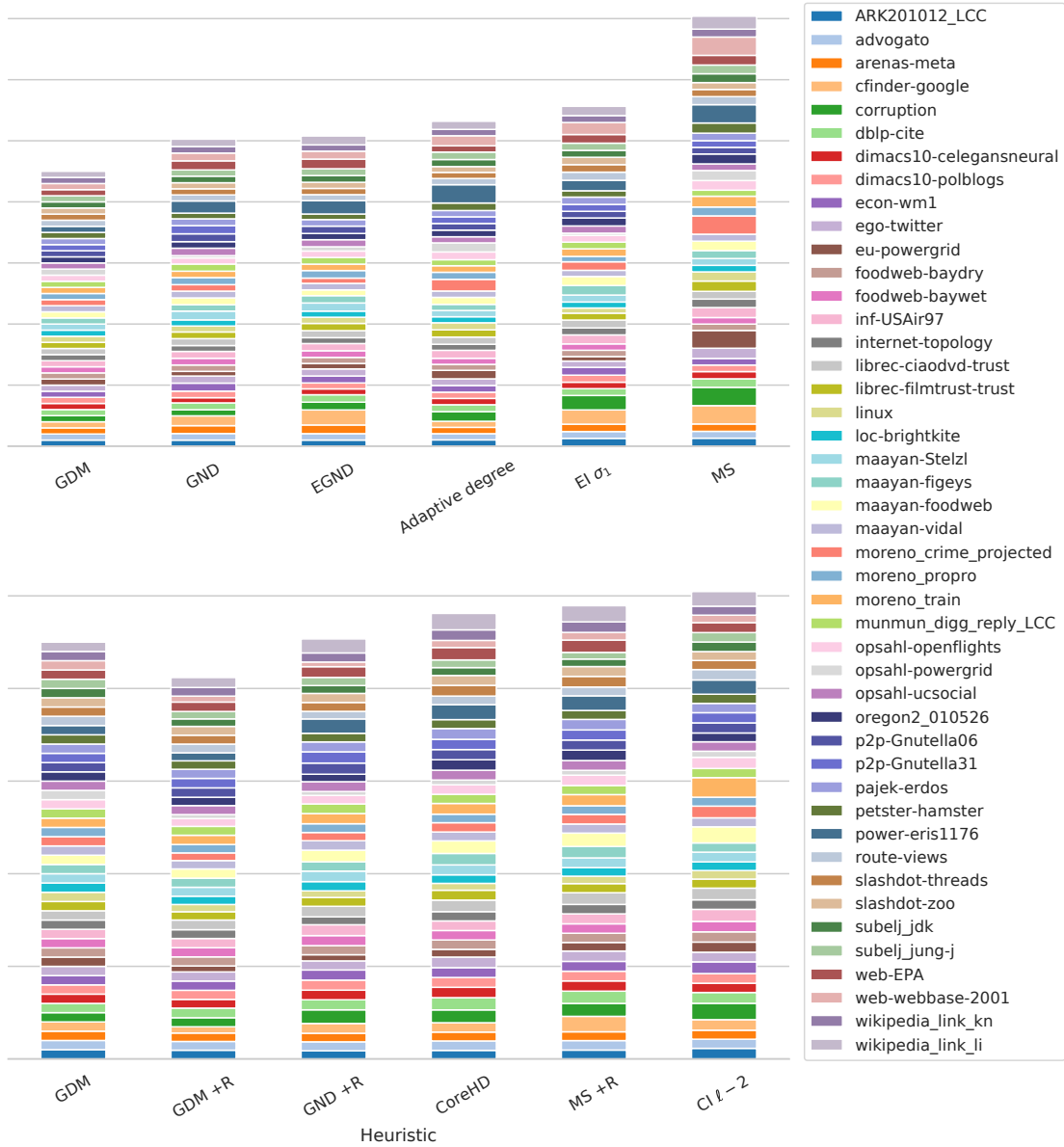
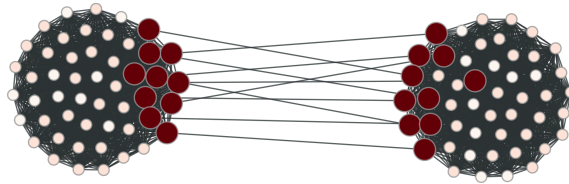
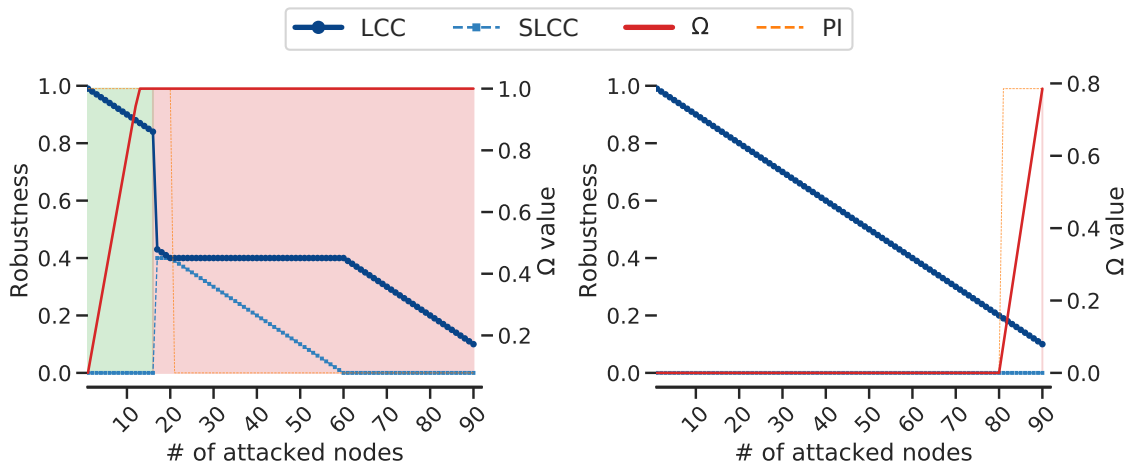


Figure 3: **Dismantling empirical complex systems.** Per-method cumulative area under the curve (AUC) of real-world networks dismantling. The lower the better. The dismantling target for each method is 10% of the network size. Each value is scaled to the one of our approach (GDM) for the same network. *GND* stands for *Generalized Network Dismantling* (with cost matrix $\mathbf{W} = \mathbf{I}$), *MS* stands for *Min-Sum*, *EI* stands for *Explosive Immunization* and *CI* for *Collective Influence*. +R means that the reinsertion phase is performed. *CoreHD* and *CI* are compared to other +R algorithms as they include the reinsertion phase. Also, note that some values are clipped (limited) to 3x for the *MS* heuristic to improve visualization.



(a) Toy-example network composed of two cliques connected by 10 bridges. The size of the nodes represents their betweenness value and the color (from dark red to white) represents their importance to the system's health according to our method.



(b) Degree or betweenness based attack.

(c) Inverse degree or betweenness based attack.

Figure 4: Toy-example meant to explain why the LCC is not sufficient to evaluate the state of the system. The LCC decreases at the same rate during the initial part of both the attacks shown. Instead, Ω values do not and reach warning levels before the system suddenly collapses.

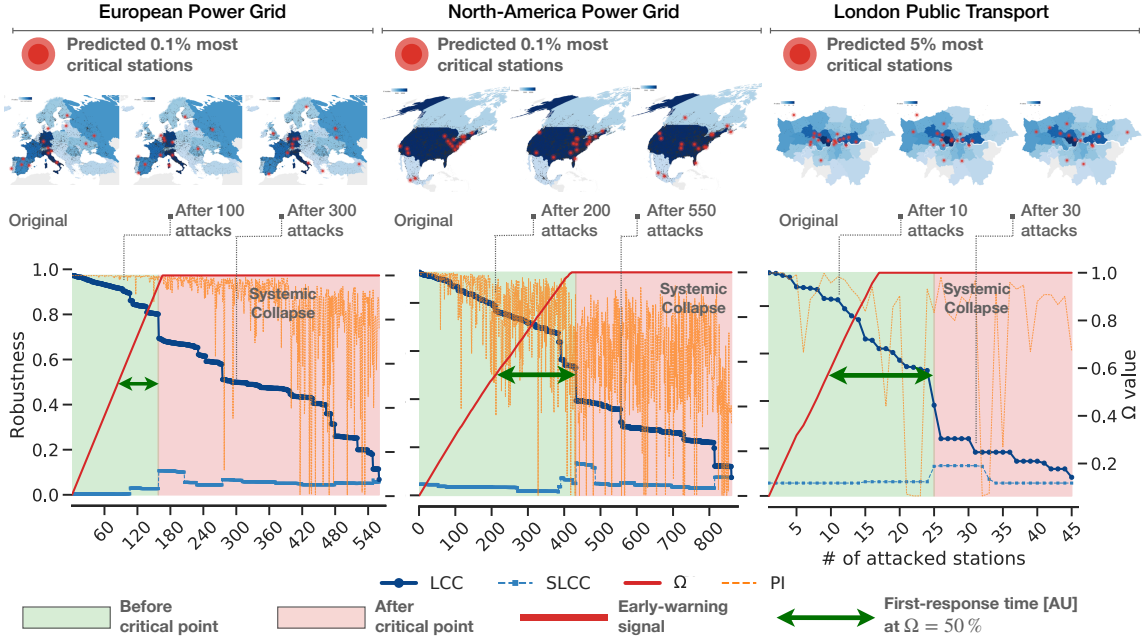


Figure 5: **Early warning due to network dismantling of real infrastructures.** Three empirical systems, namely the European power grid (left), the North-American power grid (middle) and the London public transport (right), are repeatedly attacked using a degree-based heuristics, i.e., hubs are damaged first. A fraction of the most vulnerable stations is shown for the original systems and some representative damaged states (i.e., before and after the critical point for system’s collapse), in the top of the figure. The plots show the behavior of the largest (LCC) and second-largest (SLCC) connected components, as well as the behavior of Ω , the Early Warning descriptor introduced in this study and the p_n value of each removed node (PI). Transitions between green and red areas indicate the percolation point of the corresponding systems, found through the SLCC peak. We also show the first response time in arbitrary units (AU), to highlight how our framework allows to anticipate system’s collapse, allowing for timely emergency response.

Machine learning dismantling and early-warning signals of disintegration in complex systems

Marco Grassia¹, Manlio De Domenico^{2*}, Giuseppe Mangioni^{1*}

¹Dip. Ingegneria Elettrica, Elettronica e Informatica - Università degli Studi di Catania - Italy

²CoMuNe Lab, Fondazione Bruno Kessler, Via Sommarive 18, 38123 Povo (TN), Italy

*To whom correspondence should be addressed;

E-mail: giuseppe.mangioni@dieei.unict.it; mdedomenico@fbk.eu.

Supplementary Materials

Here, we provide additional examples and details about the results we discussed in the main text. We begin detailing the architecture of the employed deep learning model and the way it is trained. Secondly, we discuss the computational complexity of our framework and then we show more toy and real-world examples on the dismantling process and on the Early Warning Ω . Lastly, we list the test networks used to evaluate our approach.

Deep Learning Model

How the model works A simplistic but more practical understanding of how a model with L GAT network layers assigns the p_n value to each node n can be achieved by considering the L -hop neighborhood of the node. Consider a tree with height L with node n as root and where each node's neighbors are its children. That is, each level $l + 1$ of the tree is populated with the neighbors of nodes at level l . For instance, at level 1 we have n 's neighbors.

Now, n 's high-level node features (h_n^L) are computed by aggregating the information from the L -hop neighborhood in a bottom up fashion. Each GAT network layer processes a level of the tree, so the deeper the model, the farther the information comes from. That is, the model starts from the bottom of the tree (i.e., the nodes at L hops from n) to compute the high-level node features of each node at layer L and goes up until the root (node n) is reached.

This means that the model is able to aggregate the information in the whole n 's L -hop neighborhood in h_n^L , which also accounts for the different importance each node has in that neighborhood thanks to the GAT's self-attention mechanism. The basic idea is somehow similar to the *Collective Influence* approach, with the main differences being that the geometric deep learning model learns a weighted sum function from the training data to aggregate many node features, whereas the *Collective Influence* just sums the degrees, and also that the model aggregates the whole L -hop neighborhood ball, not just its frontier.

These high-level features (h_n^L) are then fed to a regressor that returns p_n , the node's structural importance indicator used in our work.

The actual implementation of our model relies on *PyTorch Geometric* library (63) on-top of *PyTorch* (90), while the handling of the graphs (i.e., implementation of the data structures, removal of the nodes and the computation of the connected components) is performed using *graph-tool* (91).

Training We train our models in a supervised manner. Our training data is composed of small synthetic networks (25 nodes each) generated using the Barabási-Albert (BA), the Erdős-Rényi (ER) and the Static Power law generational models that are implemented in *iGraph* (58) and *NetworkX* (67). Each synthetic network is dismantled optimally using brute-force and nodes are assigned a numeric label (the learning target) that depends on their presence in the optimal dismantling set(s). That is, all combinations of increasing length of nodes are removed until we

find at least one that shrinks the Largest Connected Component (LCC) to a given target size, $\sim 18\%$ in our tests; then, the label of each node is computed as the number of optimal sets it belongs to, divided by the total number of optimal sets. For example, if there is only a set of optimal size, we assign a label value of 1 to the nodes in that set and 0 to all other nodes. This is meant to teach the model that some nodes are more critical than others since they belong to many optimal dismantling sets.

We stress that the training label is arbitrary and others may work better for other training sets or targets. Moreover, while we train on a generic purpose dataset that includes both power law and ER networks, the training networks can also be chosen to fit the target networks, e.g., by using networks from similar domains or with similar characteristics.

Node features Considering that the model can process any features combination, one could just choose to stuff every suitable node metrics that comes to his mind and, since it is proven that Deep Neural Networks learn the feature importance, let them do the rest. On the other hand, it could also be tempting to use no features at all (e.g, a constant value for every node) since Kipf et al. (72) showed that their *Graph Convolutional Network (GCN)*, a particular type of convolutional-style graph neural networks, can learn to linearly separate the communities based on the network structure alone and on minimal supervision (one labelled node per community), meaning that convolutional-style neural networks can leverage the network topology to assign a higher-level node feature that describes its role in the network.

We argue that, while the first idea could make sense for scenarios where training data is abundant and the features are cheap to compute, and while the second shows worse (with respect to models with simple features) but still interesting performance, it makes sense to perform some feature selection a priori to keep the computational complexity of the attack low and also to speed-up the learning process. With that in mind, we pick node degree (plus its *Pearson's*

chi-square statistic, χ^2 , over the neighborhood), *k*-coreness and local clustering coefficient as node features.

Parameters We run a grid search to test various combination of model parameters, which are reported here, and select the models that better fit the dismantling target (i.e., lower area under the curve or lower number of removals).

- Convolutional-style layers: *Graph Attention Network* layers.
 - Number of layers: from 1 to 4;
 - Output channels for each layer: 5, 10, 20, 30, 40 or 50, sometimes with a decreasing value between consecutive layers;
 - Multi-head attentions: 1, 5, 10, 15, 20 or 30 concatenated heads;
 - Dropout probability: fixed to 0.3;
 - Leaky ReLU angle of the negative slope: fixed to 0.2;
 - Each layer learns an additive bias;
 - Each layer is coupled with a linear layer with the same number of input and output channels;
 - Activation function: Exponential Linear Unit (ELU). The input at each convolutional layer is the sum between the output of the GAT and the linear layers;

- Regressor: Multi Layer Perceptron
 - Number of layers: from 1 to 4;
 - Number of neurons per layer: 20, 30, 40, 50 or 100, sometimes with a decreasing value between consecutive layers.

- Learning rate: fixed to 10^{-5} ;
- Epochs: we train each model for 50 epochs;

Computational complexity

The computational complexity of our approach mainly depends on two elements: 1) the computational complexity of the node features used and 2) the computational complexity of the convolutional-style layers in the model. In particular, the convolutional-style layers that we employ, i.e., the *Graph Attention Network*, scale as $O(N + E)$ where N is the number of nodes and E is the number of edges in the network. Considering that real-world networks are usually sparse, we assume that $O(E) \approx O(N)$, so $O(N + E) \approx O(N)$, and the computational complexity of our approach is the maximum between this and the computational complexity of the features. Given that, the most expensive feature we compute in our experiments is the k -coreness, that is $O(N + E)$, so the computational complexity of the approach detailed above is $O(N)$. For what concerns the computational complexity of the brute-force performed during the training set generation, it is irrelevant as it is a highly parallelizable one-time task that is performed on very small networks. Moreover, since the neural models can generalize, there is no need to train them for each dismantling, and the actual time spent training is negligible.

Other Results

Understanding GDM’s behavior Before testing on real-world networks, we investigate the behavior of our approach by dismantling some toy-example networks. To this aim, we employ the same low computational complexity node features from the main paper (that are also detailed above).

The first toy example, shown in figure 1a, is a network built from three ego-networks joined

by a bridge. The betweenness based heuristics¹, and also our common sense, would suggest to remove the bridge first, reducing the LCC size to one third of the initial value, and then remove the nodes at the center of the unconnected ego networks left, for a total of four removals. Instead, our model predicts a different strategy and removes only the cores of the ego sub-networks, reaching the same LCC size with just three removals, as shown in Figure 2a.

At this point, we want to probe if the model is just learning to remove the nodes in descending degree order as the previous example would suggest. If that is the case, in our second toy example network, composed of a clique with an appended tail as illustrated in Figure 1b, the model would remove the nodes in the clique first, given their high degree. Instead, the tail is detached first, meaning that the predicted strategy differs from the degree based one, and both the degree and betweenness-based heuristics are outperformed, as shown in Figure 2b.

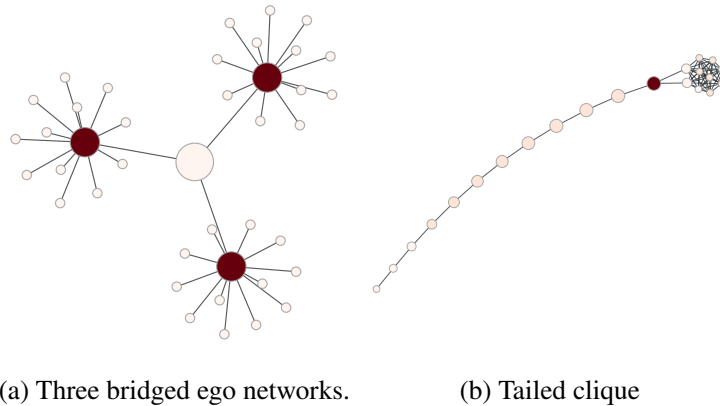


Figure 1: Toy examples. The color of the nodes represents (from dark red to white) the removal order of predicted strategy, while their size represents their betweenness value.

Dismantling real-world complex systems

¹The removal of nodes by descending betweenness centrality order. The node betweenness is a node centrality measure that captures the importance of the node to the shortest paths through the network.

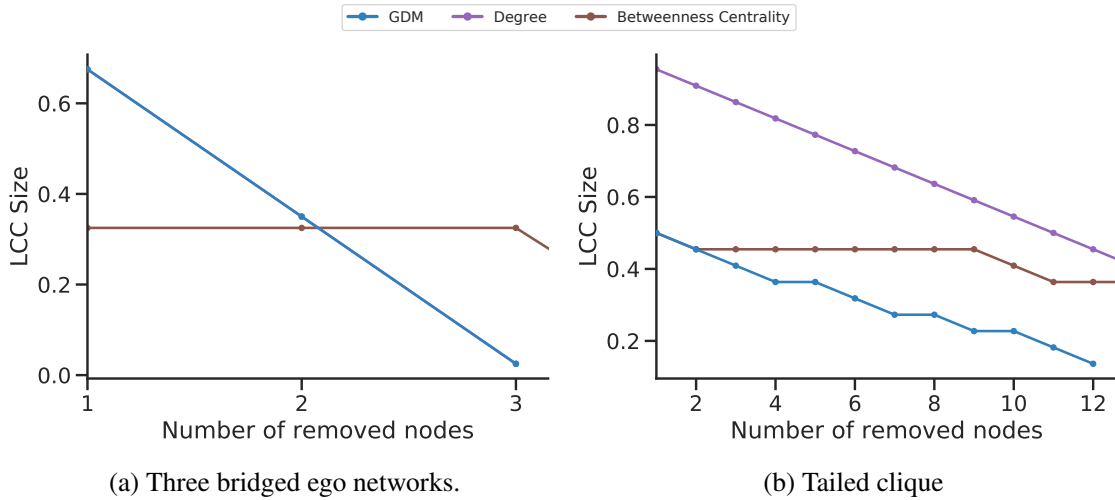


Figure 2: Dismantling the toy example networks using our approach, GDM, and the degree and betweenness based heuristics as comparison.

Enhancement of metric-based heuristics In order to better understand how our framework is able to outperform cutting-edge algorithms, we compare existing node metric-based heuristics (e.g., removal of nodes in degree order) against GDM models that employ the corresponding node metric as the only node feature. As an example, in Figure 3 we display the enhancement of the degree and the betweenness based heuristics in the left and right columns respectively. These GDM-enhanced heuristics effectively outperform the vanilla ones, highlighting the fact that the model is able to capture the importance of the nodes thanks to the feature propagation discussed before. This also gives an important insight as the model seems to learn correlations between node features.

Dismantling of configuration model rewired networks We investigate further if the model is learning correlations among node features by dismantling the configuration model rewirings² of the networks in our test set. If that is the case, the dismantling power of our ap-

²The configuration model of a network keeps the observed connectivity distribution while destroying topological correlations, meaning that feature correlations are lost.

proach on the rewirings should be heavily affected. In Figure 4 we show, for each network, the dismantling of 1000 configuration models and also the original instance as comparison. In all the tested networks, there is a severe performance drop. For instance, in Figures 4b it takes just ~ 35 removals to dismantle the original instance of the Moreno crime network, while the LCC size of the rewired networks after the same number of removals is still very large (i.e., $\sim 95\%$). This result confirms our insight. That is, existing topological correlations are learned and, consequently, exploited by the machine.

Dismantling results In the main paper we compare our approach with the state-of-the-art algorithms. In Table 1 we report the same results in numerical form.

The table also includes other commonly used static attack approaches that remove the nodes in descending importance order according to some node centrality metric. While many heuristics fall in this category, we compare with the removal of nodes in descending degree (71), betweenness (71) and PageRank (88). Our approach outperforms all these static approaches with a significant margin, even the ones with higher computational complexity (e.g., the betweenness-based one).

Dismantling of large networks While in the main paper we compare our approach on small and medium size networks, in this section we extend the comparison against the more promising state-of-the-art algorithms (*GND* and *MS* with and without reinsertion, and *CoreHD*) to 12 large networks with up to 1.8M nodes and up to 2.8M edges.

As shown in Figure 5 and in Table 2, the results from the main paper are confirmed even for these networks, although with smaller margins. This is still impressive as the proposed approach is static while the others recompute the nodes’ structural importance during the dismantling process, which involves many removals for these networks (e.g., 70K on *hyves* network) and changes the network topology drastically, confirming the validity of our approach.

In Table 3, we also report the prediction (if any) and dismantling time of each of the above mentioned methods to give a better idea on what their different computational complexities mean and translate into.

Dismantling curves In Figure 6, we display the dismantling of most of our test networks and compare with the state-of-the-art algorithms and with the heuristics introduced in the previous paragraph. As previously mentioned, one of the advantages of our approach is that we can choose the best model to reach a given objective. As an example, we show the models that lower the area under the curve (GDM AUC) and the removals number (GDM #Removals), which may overlap for some networks. We also show the dismantling performing the reinsertion phase and compare with state-of-the-art algorithms in Figure 7.

More Early Warning Ω examples In addition to the example applications of Ω illustrated in the main paper, we also test if it can detect the collapse of other systems. In particular, we show the SciKit European powergrid (eu-powergrid) under random failures, degree or Min-Sum + Reinsertion phase attacks in Figure 8, and also various American roads under Generalized Network Dismantling + Reinsertion phase attacks in Figure 9. In all these scenarios, Ω is able to detect the system damage and reaches warning levels before the system collapse actually happens, even in case of multiple large connected components detaching from the larger one as the attack goes on.

Dataset

In Table 4 we list the test networks used in our experiments with their category and size (number of nodes and edges). Those networks model systems from various domains (e.g., biological, infrastructure and social data and so on), and range from a few hundred of nodes to more than one million. For more about each network, we refer the reader to the original source.

Test environment

Here we detail the environment where our experiments were performed and the tools used.

All experiments ran on a shared machine equipped with two Intel Xenon E5-2620 CPUs, 128GB RAM and a two core nVidia Tesla K80 (with 12GB VRAM each). More details about the drivers used and the full package dependency list of our code can be found in the code package.

Concerning the other algorithms used in our comparison (i.e., *GND*, *EGND MS*, *CoreHD* and *EI*), we use authors' official code with default parameters. Specifically, we use identity weight input matrix for both *GND* and *EGND* (and the relative fine-tuning algorithm), 1*K* trials for the *EGND*.

References

1. Jdk dependency network dataset – KONECT, September 2016.
2. Advogato network dataset – KONECT, April 2017.
3. Brightkite network dataset – KONECT, April 2017.
4. Caenorhabditis elegans network dataset – KONECT, April 2017.
5. Catster/dogster familylinks/friendships network dataset – KONECT, April 2017.
6. Citeseer network dataset – KONECT, April 2017.
7. Crime network dataset – KONECT, April 2017.
8. Dblp co-authorship network dataset – KONECT, April 2017.
9. Dblp network dataset – KONECT, April 2017.

10. Digg friends network dataset – KONECT, April 2017.
11. Digg network dataset – KONECT, October 2017.
12. Douban network dataset – KONECT, April 2017.
13. Eu institution network dataset – KONECT, April 2017.
14. Florida ecosystem dry network dataset – KONECT, April 2017.
15. Florida ecosystem wet network dataset – KONECT, April 2017.
16. Gnutella network dataset – KONECT, April 2017.
17. Google.com internal network dataset – KONECT, April 2017.
18. Gowalla network dataset – KONECT, April 2017.
19. Hamsterster full network dataset – KONECT, April 2017.
20. Human protein (figeys) network dataset – KONECT, April 2017.
21. Human protein (stelzl) network dataset – KONECT, April 2017.
22. Human protein (vidal) network dataset – KONECT, April 2017.
23. Hyves network dataset – KONECT, April 2017.
24. Internet topology network dataset – KONECT, April 2017.
25. Jung and javax dependency network dataset – KONECT, April 2017.
26. Linux network dataset – KONECT, April 2017.
27. Little rock lake network dataset – KONECT, April 2017.

28. Notre dame network dataset – KONECT, April 2017.
29. Openflights network dataset – KONECT, April 2017.
30. Protein network dataset – KONECT, April 2017.
31. Route views network dataset – KONECT, April 2017.
32. Slashdot threads network dataset – KONECT, April 2017.
33. Slashdot zoo network dataset – KONECT, April 2017.
34. Stanford network dataset – KONECT, April 2017.
35. Train bombing network dataset – KONECT, April 2017.
36. Twitter (icwsm) network dataset – KONECT, October 2017.
37. Twitter lists network dataset – KONECT, April 2017.
38. Uc irvine messages network dataset – KONECT, April 2017.
39. Us power grid network dataset – KONECT, April 2017.
40. Wordnet network dataset – KONECT, April 2017.
41. Caenorhabditis elegans (neural) network dataset – KONECT, January 2018.
42. Ciaodvd trust network dataset – KONECT, January 2018.
43. Erdős network dataset – KONECT, March 2018.
44. Filmtrust trust network dataset – KONECT, January 2018.
45. Political blogs network dataset – KONECT, January 2018.

46. Wikipedia links (kn) network dataset – KONECT, January 2018.
47. Wikipedia links (li) network dataset – KONECT, January 2018.
48. Lada A. Adamic and Natalie Glance. The political blogosphere and the 2004 US election: Divided they blog. In *Proc. Int. Workshop on Link Discov.*, pages 36–43, 2005.
49. Reka Albert, Hawoong Jeong, and Albert-Laszlo Barabási. Internet: Diameter of the world-wide web. *Nature*, 401(6749):130–131, Sep 1999.
50. Vladimir Batagelj and Andrej Mrvar. Pajek datasets, July.
51. Kurt Bollacker, Steve Lawrence, and C. Lee Giles. CiteSeer: An autonomous Web agent for automatic retrieval and identification of interesting publications. In *Proc. Int. Conf. on Autonomous Agents*, pages 116–123, 1998.
52. Thomas Brinkhoff. A framework for generating network-based moving objects. *GeoInformatica*, 6, 06 2000.
53. CAIDA. Ipv4 routed /24 as links dataset.
54. Eunjoon Cho, Seth A. Myers, and Jure Leskovec. Friendship and mobility: User movement in location-based social networks. In *Proc. Int. Conf. on Knowledge Discovery and Data Mining*, pages 1082–1090, 2011.
55. Munmun De Choudhury, Yu-Ru Lin, Hari Sundaram, K. Selçuk Candan, Lexing Xie, and Aisling Kelliher. How does the data sampling strategy impact the discovery of information diffusion in social media? In *ICWSM*, pages 34–41, 2010.
56. Munmun De Choudhury, Hari Sundaram, Ajita John, and Dorée Duncan Seligmann. Social synchrony: Predicting mimicry of user actions in online social media. In *Proc. Int. Conf. on Comput. Science and Engineering*, pages 151–158, 2009.

57. Stéphane Coulomb, Michel Bauer, Denis Bernard, and Marie-Claude Marsolier-Kergoat. Gene essentiality and the topology of protein interaction networks. *Proceedings of the Royal Society B: Biological Sciences*, 272(1573):1721–1725, 2005.
58. Gabor Csardi and Tamas Nepusz. The igraph software package for complex network research. *InterJournal, Complex Systems*:1695, 2006.
59. Manlio De Domenico, Albert Solé-Ribalta, Sergio Gómez, and Alex Arenas. Navigability of interconnected networks under random failures. *Proceedings of the National Academy of Sciences*, 111(23):8351–8356, 2014.
60. Jordi Duch and Alex Arenas. Community detection in complex networks using extremal optimization. *Phys. Rev. E*, 72(2):027104, 2005.
61. Rob M. Ewing, Peter Chu, Fred Elisma, Hongyan Li, Paul Taylor, Shane Climie, Linda McBroom-Cerajewski, Mark D. Robinson, Liam O’Connor, Michael Li, Rod Taylor, Moyez Dharsee, Yuen Ho, Adrian Heilbut, Lynda Moore, Shudong Zhang, Olga Ornatsky, Yury V. Bukhman, Martin Ethier, Yinglun Sheng, Julian Vasilescu, Mohamed Abu-Farha, Jean-Philippe P. Lambert, Henry S. Duewel, Ian I. Stewart, Bonnie Kuehl, Kelly Hogue, Karen Colwill, Katharine Gladwish, Brenda Muskat, Robert Kinach, Sally-Lin L. Adams, Michael F. Moran, Gregg B. Morin, Thodoros Topaloglou, and Daniel Figeys. Large-scale mapping of human protein–protein interactions by mass spectrometry. *Molecular Systems Biology*, 3, 2007.
62. Christiane Fellbaum, editor. *WordNet: an Electronic Lexical Database*. MIT Press, 1998.
63. Matthias Fey and Jan E. Lenssen. Fast graph representation learning with PyTorch Geometric. In *ICLR Workshop on Representation Learning on Graphs and Manifolds*, 2019.

64. Guobing Guo, Jia Zhang, and Neil Yorke-Smith. A novel Bayesian similarity measure for recommender systems. In *Proc. Int. Joint Conf. on Artif. Intell.*, pages 2619–2625, 2013.
65. Guobing Guo, Jie Zhang, Daniel Thalmann, and Neil Yorke-Smith. ETAF: An extended trust antecedents framework for trust prediction. In *Proc. Int. Conf. Adv. in Soc. Netw. Anal. and Min.*, pages 540–547, 2014.
66. Vicenç Gómez, Andreas Kaltenbrunner, and Vicente López. Statistical analysis of the social network and discussion threads in Slashdot. In *Proc. Int. World Wide Web Conf.*, pages 645–654, 2008.
67. Aric A. Hagberg, Daniel A. Schult, and Pieter J. Swart. Exploring network structure, dynamics, and function using NetworkX. In *Proceedings of the 7th Python in Science Conference (SciPy2008)*, pages 11–15, Pasadena, CA USA, August 2008.
68. Jing-Dong J Han, Denis Dupuy, Nicolas Bertin, Michael E Cusick, and Marc Vidal. Effect of sampling on topology predictions of protein-protein interaction networks. *Nature Biotechnology*, 23(7):839–844, 2005.
69. Brian Hayes. Connecting the dots. can the tools of graph theory and social-network studies unravel the next big plot? *American Scientist*, 94(5):400–404, 2006.
70. T. Hogg and K. Lerman. Social dynamics of Digg. *EPJ Data Science*, 1(5), 2012.
71. Petter Holme, Beom Jun Kim, Chang No Yoon, and Seung Kee Han. Attack vulnerability of complex networks. *Phys. Rev. E*, 65:056109, May 2002.
72. Thomas N Kipf and Max Welling. Semi-supervised classification with graph convolutional networks. *arXiv preprint arXiv:1609.02907*, 2016.

73. Jérôme Kunegis, Andreas Lommatzsch, and Christian Bauckhage. The Slashdot Zoo: Mining a social network with negative edges. In *Proc. Int. World Wide Web Conf.*, pages 741–750, 2009.
74. Jure Leskovec, Jon Kleinberg, and Christos Faloutsos. Graphs over time: Densification laws, shrinking diameters and possible explanations. In *Proceedings of the Eleventh ACM SIGKDD International Conference on Knowledge Discovery in Data Mining, KDD '05*, page 177–187, New York, NY, USA, 2005. Association for Computing Machinery.
75. Jure Leskovec, Jon Kleinberg, and Christos Faloutsos. Graph evolution: Densification and shrinking diameters. *ACM Trans. Knowledge Discovery from Data*, 1(1):1–40, 2007.
76. Jure Leskovec and Andrej Krevl. SNAP Datasets: Stanford large network dataset collection, June 2014.
77. Jure Leskovec, Kevin Lang, Anirban Dasgupta, and Michael W. Mahoney. Community structure in large networks: Natural cluster sizes and the absence of large well-defined clusters. *Internet Mathematics*, 6(1):29–123, 2009.
78. Michael Ley. The DBLP computer science bibliography: Evolution, research issues, perspectives. In *Proc. Int. Symposium on String Processing and Information Retrieval*, pages 1–10, 2002.
79. Feifei Li, Dihan Cheng, Marios Hadjieleftheriou, George Kollios, and Shang-Hua Teng. On trip planning queries in spatial databases. In Claudia Bauzer Medeiros, Max J. Egenhofer, and Elisa Bertino, editors, *Advances in Spatial and Temporal Databases*, pages 273–290, Berlin, Heidelberg, 2005. Springer Berlin Heidelberg.
80. Penn State University Libraries. Digital chart of the world server, 2006.

81. Neo D. Martinez, John J. Magnuson, Timothy. Kratz, and M. Sierszen. Artifacts or attributes? effects of resolution on the Little Rock Lake food web. *Ecological Monographs*, 61:367–392, 1991.
82. Paolo Massa, Martino Salvetti, and Danilo Tomasoni. Bowling alone and trust decline in social network sites. In *Proc. Int. Conf. Dependable, Autonomic and Secure Computing*, pages 658–663, 2009.
83. Carsten Matke, Wided Medjroubi, and David Kleinhans. SciGRID - An Open Source Reference Model for the European Transmission Network (v0.2), Jul 2016.
84. Julian McAuley and Jure Leskovec. Learning to discover social circles in ego networks. In *Advances in Neural Information Processing Systems*, pages 548–556. 2012.
85. Flaviano Morone and Hernán A Makse. Influence maximization in complex networks through optimal percolation. *Nature*, 524(7563):65, 2015.
86. Tore Opsahl, Filip Agneessens, and John Skvoretz. Node centrality in weighted networks: Generalizing degree and shortest paths. *Social Networks*, 3(32):245–251, 2010.
87. Tore Opsahl and Pietro Panzarasa. Clustering in weighted networks. *Social Networks*, 31(2):155–163, 2009.
88. Lawrence Page, Sergey Brin, Rajeev Motwani, and Terry Winograd. The pagerank citation ranking: Bringing order to the web. Technical report, Stanford InfoLab, 1999.
89. Gergely Palla, Illés J. Farkas, Péter Pollner, Imre Derényi, and Tamás Vicsek. Directed network modules. *New J. Phys.*, 9(6):186, 2007.

90. Adam Paszke, Sam Gross, Soumith Chintala, Gregory Chanan, Edward Yang, Zachary DeVito, Zeming Lin, Alban Desmaison, Luca Antiga, and Adam Lerer. Automatic differentiation in pytorch. 2017.
91. Tiago P. Peixoto. The graph-tool python library. *figshare*, 2014.
92. Haroldo V Ribeiro, Luiz G A Alves, Alvaro F Martins, Ervin K Lenzi, and Matjaž Perc. The dynamical structure of political corruption networks. *Journal of Complex Networks*, 6(6):989–1003, 01 2018.
93. Matei Ripeanu, Ian Foster, and Adriana Iamnitchi. Mapping the Gnutella network: Properties of large-scale peer-to-peer systems and implications for system design. *IEEE Internet Comput. J.*, 6, 2002.
94. Ryan A. Rossi and Nesreen K. Ahmed. The network data repository with interactive graph analytics and visualization. In *AAAI*, 2015.
95. Jean-François Rual, Kavitha Venkatesan, Tong Hao, Tomoko Hirozane-Kishikawa, Amélie Dricot, Ning Li, Gabriel F. Berriz, Francis D. Gibbons, Matija Dreze, and Nono Ayivi-Guedehoussou. Towards a proteome-scale map of the human protein–protein interaction network. *Nature*, (7062):1173–1178, 2005.
96. U. Stelzl, U. Worm, M. Lalowski, C. Haenig, F. H. Brembeck, H. Goehler, M. Stroedicke, M. Zenkner, A. Schoenherr, S. Koeppen, J. Timm, S. Mintzlaff, C. Abraham, N. Bock, S. Kietzmann, A. Goedde, E Toksöz, A. Droege, S. Krobitsch, B. Korn, W. Birchmeier, H. Lehrach, and E. E. Wanker. A human protein–protein interaction network: A resource for annotating the proteome. *Cell*, 122:957–968, 2005.

97. Michael PH Stumpf, Carsten Wiuf, and Robert M May. Subnets of scale-free networks are not scale-free: Sampling properties of networks. *Proceedings of the National Academy of Sciences of the United States of America*, 102(12):4221–4224, 2005.
98. Robert E. Ulanowicz, Johanna J. Heymans, and Michael S. Egnotovitch. Network analysis of trophic dynamics in South Florida ecosystems, FY 99: The graminoid ecosystem. *Annual Report to the United States Geological Service Biological Resources Division Ref. No.[UMCES] CBL 00-0176, Chesapeake Biological Laboratory, University of Maryland*, 2000.
99. Lovro Šubelj and Marko Bajec. Software systems through complex networks science: Review, analysis and applications. In *Proc. Int. Workshop on Software Mining*, pages 9–16, 2012.
100. Duncan J. Watts and Steven H. Strogatz. Collective dynamics of ‘small-world’ networks. *Nature*, 393(1):440–442, 1998.
101. John G. White, E. Southgate, J. N. Thomson, and S. Brenner. The structure of the nervous system of the nematode *Caenorhabditis elegans*. *Phil. Trans. R. Soc. Lond*, 314:1–340, 1986.
102. Bart Wiegmans. Gridkit: European and north-american extracts, Mar 2016.
103. Jaewon Yang and Jure Leskovec. Defining and evaluating network communities based on ground-truth. In *Proc. ACM SIGKDD Workshop on Mining Data Semantics*, page 3. ACM, 2012.
104. R. Zafarani and H. Liu. Social computing data repository at ASU, 2009.

105. Beichuan Zhang, Raymond Liu, Daniel Massey, and Lixia Zhang. Collecting the Internet AS-level topology. *SIGCOMM Computer Communication Review*, 35(1):53–61, 2005.

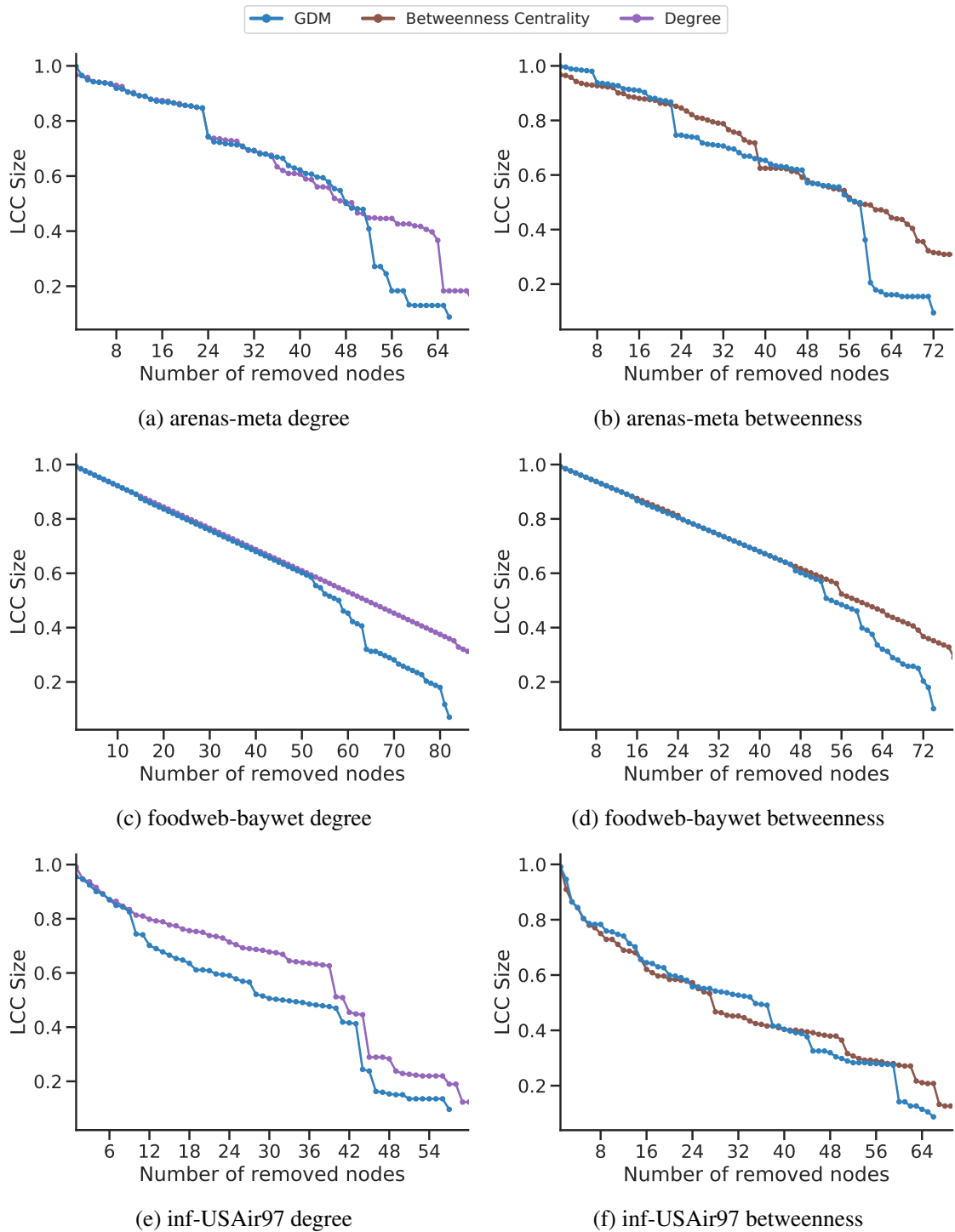


Figure 3: Comparison of degree and betweenness vanilla heuristics with their GDM-enhanced versions on the arenas-meta, foodweb-baywet and inf-USAir97 networks.

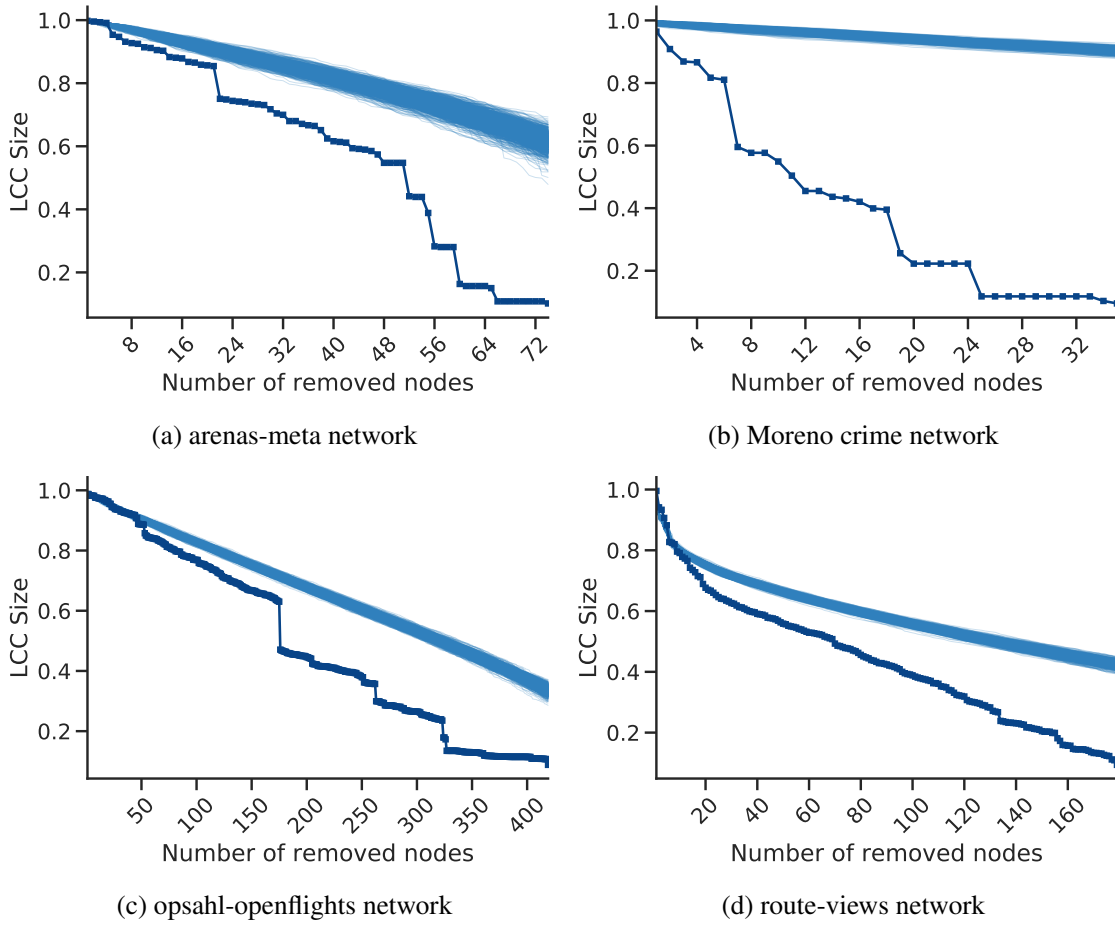


Figure 4: Dismantling of original networks (dark blue) and 1000 configuration model rewirings for each (light blue).

Heuristic Network	GDM	GND	EGND	Adaptive degree	El σ_1	Pagerank	Degree	Betweenness	MS	El σ_2	GDM +R	GND +R	CoreHD	MS +R	CI $\ell - 2$
ARK201012_LCC	100.0	99.7	100.1	103.3	128.4	103.1	104.9	123.3	130.9	3883.7	94.5	87.6	92.6	95.8	114.6
advogato	100.0	108.0	105.5	101.8	111.6	150.1	113.4	114.8	112.6	494.5	94.8	97.5	102.1	102.7	98.8
arenas-meta	100.0	129.0	141.9	103.6	120.4	114.8	116.4	142.4	120.5	579.3	90.8	92.5	95.5	94.9	96.9
cfinder-google	100.0	160.4	246.5	99.5	233.7	113.5	141.3	377.9	682.8	1609.3	67.5	105.6	101.0	166.9	114.0
corruption	100.0	99.3	126.9	157.3	236.3	147.5	400.1	166.7	864.8	1141.9	97.6	147.4	138.6	139.6	176.6
dblp-cite	100.0	113.3	121.7	113.5	111.7	114.7	131.6	119.0	139.8	533.5	103.9	108.5	132.3	132.5	117.1
dimacs10-celegansneural	100.0	85.0	95.9	103.1	105.7	116.4	120.8	125.1	117.5	182.2	94.2	103.8	111.6	110.3	99.7
dimacs10-polblogs	100.0	107.5	97.1	102.1	115.5	112.5	117.9	114.8	107.5	262.3	98.4	108.4	106.0	104.9	104.6
econ-wm1	100.0	130.3	114.4	109.8	128.0	131.0	129.4	132.7	107.7	309.3	99.6	109.4	106.0	105.9	126.3
ego-twitter	100.0	116.8	115.8	108.9	103.0	107.8	108.8	133.3	167.3	6017.4	98.8	98.2	114.4	111.7	103.9
eu-powergrid	100.0	75.9	89.1	138.8	73.8	180.1	163.5	174.5	290.9	3313.0	64.4	66.5	83.4	92.8	109.4
foodweb-baydry	100.0	104.5	99.5	98.1	103.0	120.5	122.3	109.4	104.4	125.2	97.8	98.0	101.2	99.3	110.6
foodweb-baywet	100.0	110.2	108.4	99.6	103.9	123.6	125.4	112.9	106.8	128.3	98.5	108.5	102.1	101.8	113.0
inf-USAir97	100.0	112.4	117.8	130.4	147.0	117.1	139.1	128.6	164.0	633.6	100.1	117.2	103.7	107.6	129.8
internet-topology	100.0	95.6	95.8	99.1	113.9	109.2	131.4	122.9	138.6	3879.9	94.8	84.7	100.2	101.7	103.0
librec-ciaodvd-trust	100.0	113.1	115.5	117.6	129.4	120.5	139.8	114.9	126.6	634.5	104.3	114.4	124.4	126.3	126.1
librec-filmtrust-trust	100.0	108.9	118.3	117.7	112.8	131.8	148.4	158.9	168.7	1308.2	89.7	95.5	106.8	98.6	98.0
linux	100.0	97.9	101.1	116.2	84.5	176.0	190.8	365.1	150.0	1035.2	78.3	71.4	74.1	80.1	92.1
loc-brightkite	100.0	100.2	100.3	98.6	97.7	104.3	110.9	122.1	106.7	593.9	89.5	99.7	92.1	92.4	93.0
maayan-Stelzl	100.0	144.1	133.0	102.5	114.3	113.4	127.7	137.0	111.7	1269.6	96.3	113.4	107.1	105.2	105.4
maayan-figeys	100.0	104.3	120.2	100.7	155.9	127.3	146.9	153.4	129.5	1656.6	98.0	100.1	123.7	123.4	99.5
maayan-foodweb	100.0	111.5	94.6	114.7	147.8	118.9	123.8	126.2	154.6	268.7	100.0	125.5	136.1	144.4	173.9
maayan-vidal	100.0	111.0	106.7	103.3	101.6	109.1	110.6	123.9	114.1	843.9	90.1	102.5	95.6	97.9	97.3
moreno.crime-projected	100.0	105.8	86.0	191.2	139.2	157.6	218.8	180.6	976.7	2103.3	82.7	88.8	100.3	104.1	126.2
moreno.propro	100.0	115.9	123.6	115.6	87.9	126.1	123.5	146.7	145.2	1985.3	90.7	94.6	92.2	93.1	96.3
moreno.train	100.0	104.9	104.9	107.1	124.0	149.5	156.0	134.7	176.9	408.8	100.0	109.7	115.6	120.3	211.6
munmun.digg_reply_LCC	100.0	116.3	108.6	98.5	109.4	106.5	108.3	117.5	98.9	556.8	95.6	104.0	99.0	98.4	98.5
opsahl-openflights	100.0	101.2	106.2	127.2	109.9	123.2	135.4	123.6	157.3	807.7	84.4	92.0	102.6	111.3	120.9
opsahl-powergrid	100.0	36.9	69.4	148.6	37.0	173.4	180.9	183.9	164.3	1508.1	43.1	42.1	51.4	52.5	65.6
opsahl-ucsocial	100.0	122.1	116.1	99.9	118.5	105.9	109.9	109.8	108.8	342.0	97.0	106.1	105.8	106.0	101.7
oregon2_010526	100.0	106.8	101.5	108.8	131.1	101.6	130.5	114.6	162.0	3247.5	90.0	80.5	113.0	112.8	95.1
p2p-Gnutella06	100.0	128.5	120.4	108.5	108.6	111.6	125.1	118.4	108.7	274.0	101.4	120.4	110.1	108.4	109.1
p2p-Gnutella31	100.0	133.6	NaN	109.1	112.7	110.3	123.1	129.5	109.2	474.4	102.3	121.6	110.4	108.8	109.8
pajek-erdos	100.0	112.2	107.5	103.3	119.9	103.3	104.6	106.7	122.8	2790.7	98.2	106.9	116.7	113.9	101.0
petster-hamster	100.0	92.5	90.9	122.7	103.8	135.1	127.2	123.8	166.7	402.6	91.5	93.3	96.2	96.5	98.6
power-eris1176	100.0	199.1	218.0	340.2	171.7	253.5	622.5	430.2	632.6	1957.4	86.6	154.8	161.3	157.8	153.7
route-views	100.0	99.3	99.1	101.8	133.2	103.5	103.5	112.3	131.5	4340.9	94.0	82.0	93.0	95.2	112.5
slashdot-threads	100.0	100.1	102.2	99.5	122.5	104.6	105.4	114.2	117.6	1495.8	96.1	95.8	115.7	115.1	97.9
slashdot-zoo	100.0	99.2	100.1	95.6	120.9	103.3	106.8	124.0	112.4	683.8	95.2	97.7	106.9	105.9	96.5
subelj_jdk	100.0	107.6	110.2	115.1	113.0	144.2	181.5	346.9	144.6	1275.7	80.9	84.7	84.8	81.0	103.4
subelj_jung-j	100.0	102.1	111.6	122.0	118.4	150.7	185.7	334.6	143.1	1295.0	80.1	88.5	82.9	72.2	101.5
web-EPA	100.0	148.4	157.6	102.2	141.1	104.9	109.7	137.7	158.1	1471.9	101.1	115.6	133.8	132.8	107.3
web-webbase-2001	100.0	127.6	130.0	165.0	196.6	216.3	165.4	207.7	3603.1	55066.4	64.7	50.1	76.6	82.6	80.9
wikipedia_link_kn	100.0	107.3	102.6	103.7	113.2	124.8	143.6	140.3	128.8	NaN	92.9	98.0	113.9	113.5	96.8
wikipedia_link_li	100.0	120.3	145.4	132.8	151.8	120.5	165.2	110.6	211.9	1049.4	107.2	151.0	177.5	174.5	157.8
Average	100.0	111.7	115.4	119.1	123.6	128.7	151.1	158.9	273.3	2596.4	91.5	100.8	106.9	108.7	112.1

Table 1: Per-method area under the curve (AUC) of real-world networks dismantling. The lower the better. The dismantling target for each method is 10% of the network size. We compute the AUC value by integrating the $LCC(x)/|N|$ values using Simpson’s rule, and each value is scaled to the one of our approach (GDM) for the same network. +R means that the reinsertion phase is performed. CoreHD and CI are compared to other +R algorithms as they include the reinsertion phase. EGND for p2p-Gnutella31 is missing as the computation was killed after 10d.

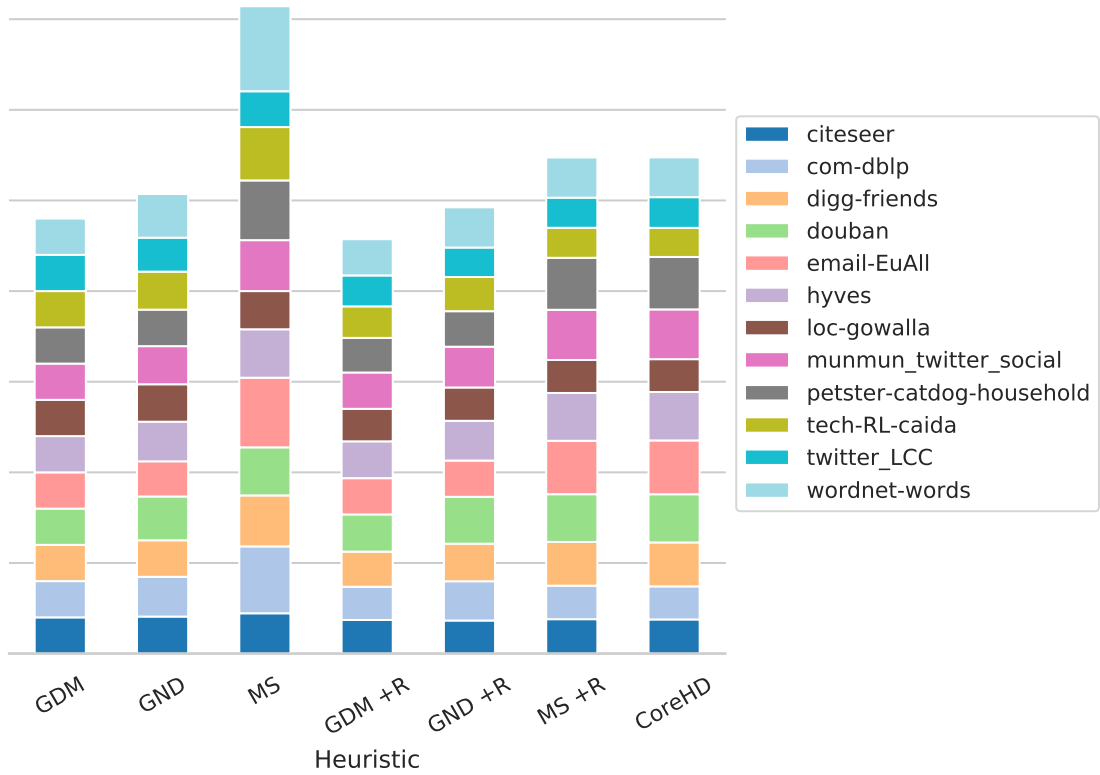


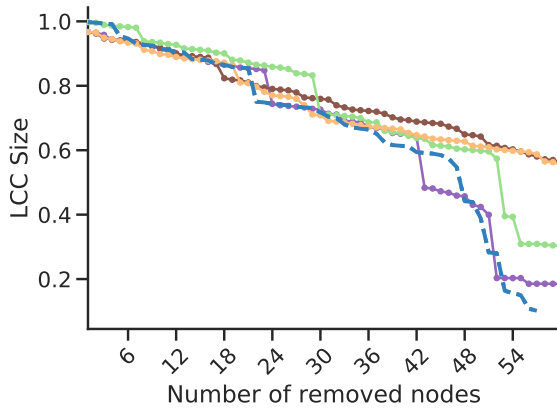
Figure 5: **Dismantling empirical complex large systems.** Per-method cumulative area under the curve (AUC) of real-world networks dismantling. The lower the better. The dismantling target for each method is 10% of the network size. We compute the AUC value by integrating the $LCC(x)/|N|$ values using Simpson’s rule, and each value is scaled to the one of our approach (GDM) for the same network. *GND* stands for *Generalized Network Dismantling* (with cost matrix $\mathbf{W} = \mathbf{I}$) and *MS* stands for *Min-Sum*. +R means that the reinsertion phase is performed. Also, note that some values are clipped (limited) to 3x for the *MS* heuristic to improve visualization.

Heuristic Network	GDM	GND	MS	GDM +R	GND +R	MS +R	CoreHD
citeseer	100.0	102.2	111.2	92.8	91.3	95.0	94.3
com-dblp	100.0	109.6	184.5	91.5	108.3	92.4	91.2
digg-friends	100.0	100.9	140.5	97.0	103.6	120.7	121.2
douban	100.0	120.8	132.7	102.6	129.3	131.6	132.9
email-EuAll	100.0	97.0	192.1	100.0	100.0	147.4	148.5
hyves	100.0	109.3	133.6	101.6	109.6	131.9	133.6
loc-gowalla	100.0	103.2	105.4	89.7	91.9	91.0	90.5
munmun_twitter_social	100.0	105.2	140.5	100.2	112.4	138.5	137.3
petster-catdog-household	100.0	100.7	164.7	95.4	98.0	143.4	144.7
tech-RL-caida	100.0	104.8	147.2	86.9	94.3	82.8	80.2
twitter_LCC	100.0	93.6	98.8	85.3	81.4	83.0	84.7
wordnet-words	100.0	120.4	234.5	100.0	110.8	111.0	109.7
Average	100.0	105.6	148.8	95.3	102.6	114.1	114.1

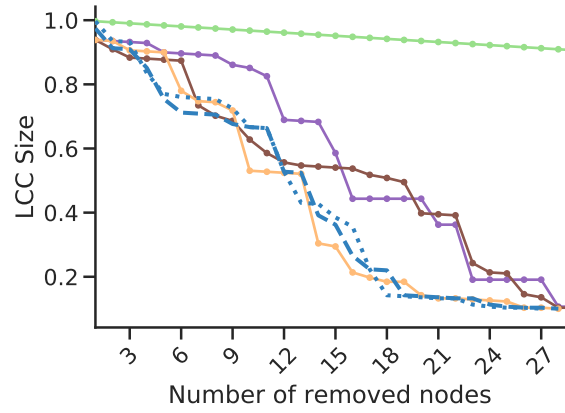
Table 2: Per-method area under the curve (AUC) of real-world large networks dismantling. The lower the better. The dismantling target for each method is 10% of the network size. We compute the AUC value by integrating the $LCC(x)/|N|$ values using Simpson’s rule, and each value is scaled to the one of our approach (GDM) for the same network. +R means that the reinsertion phase is performed. CoreHD and CI are compared to other +R algorithms as they include the reinsertion phase.

Heuristic Network	Prediction time		Dismantle time		
	GDM	CoreHD	GDM	GND	MS
citeseer	00:00:03.4	00:00:22.9	01:30:17.1	03:43:51.6	01:26:21.5
com-dblp	00:00:02.9	00:00:14.9	00:22:30.7	04:57:25.6	00:59:38.4
digg-friends	00:00:02.8	00:00:19.9	00:08:01.9	00:30:55.5	01:11:37.4
douban	00:00:01.3	00:00:06.1	00:01:10.1	00:03:34.8	00:11:40.4
email-EuAll	00:00:02.4	00:00:07.8	00:00:10.7	00:01:14.9	00:09:49.0
hyves	00:00:13.5	00:00:36.6	03:08:02.7	08:21:22.8	02:03:26.9
loc-gowalla	00:00:02.0	00:00:15.9	00:17:22.3	01:27:28.0	00:46:15.0
munmun_twitter_social	00:00:04.3	00:00:14.3	00:00:53.5	00:07:53.4	00:29:13.9
petster-catdog-household	00:00:03.9	00:00:40.6	00:44:20.5	03:58:17.1	02:16:02.8
tech-RL-caida	00:00:01.8	00:00:12.1	00:07:23.7	04:14:34.1	00:29:30.8
twitter_LCC	00:00:04.4	00:00:13.0	00:32:01.0	05:33:36.3	00:19:18.8
wordnet-words	00:00:01.4	00:00:12.1	00:03:34.0	01:23:52.1	00:22:28.5

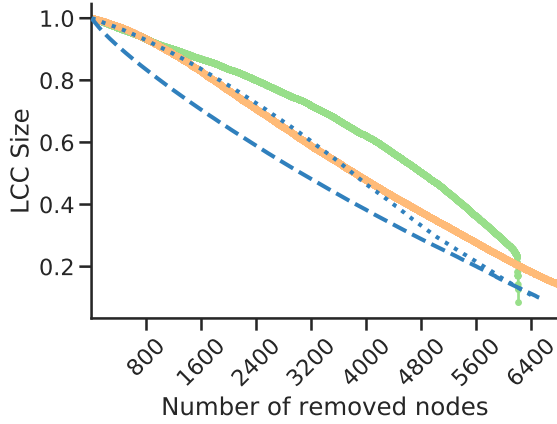
Table 3: Real-world large networks dismantling timings. The lower the better. Time format is HH:MM:SS.s. *MS* and *GND* do not have prediction time as they refresh the predictions during the dismantling, while there is no *CoreHD* dismantling column as we use our dismantler.



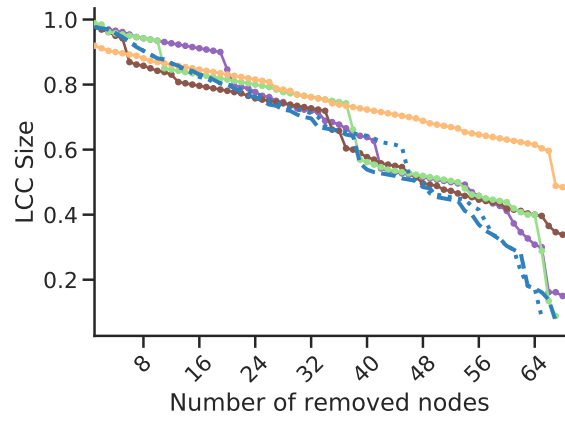
(a) arenas-meta



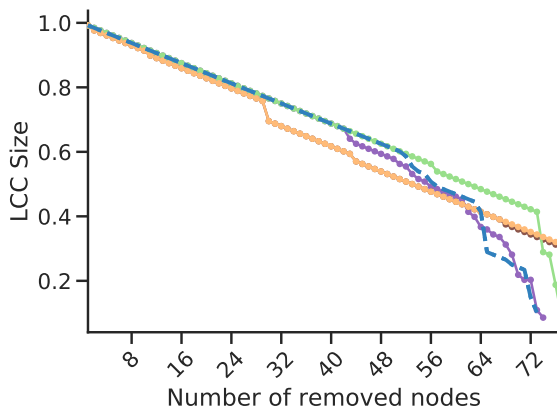
(b) corruption



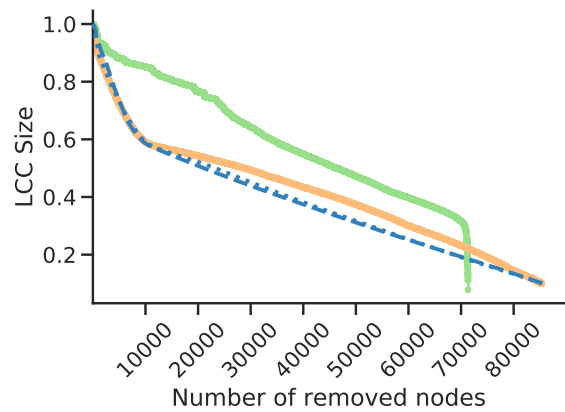
(c) douban



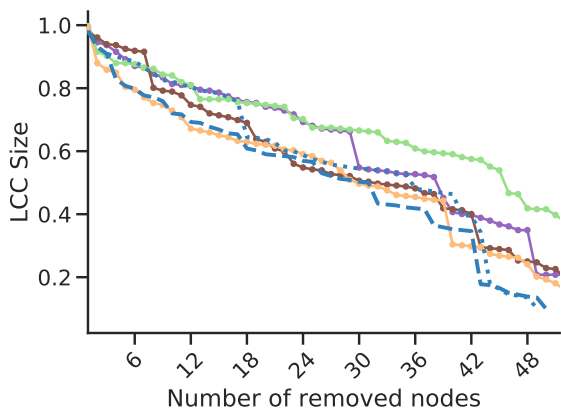
(d) econ-wm1



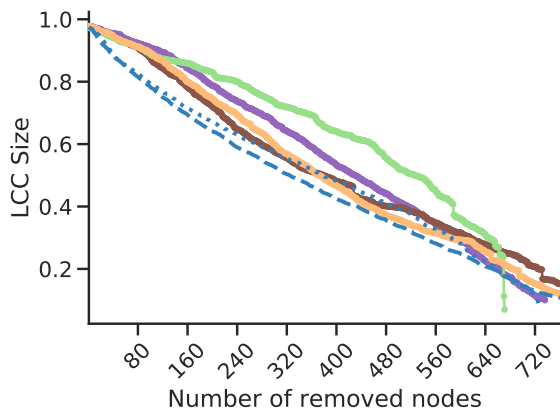
(e) foodweb-baywet



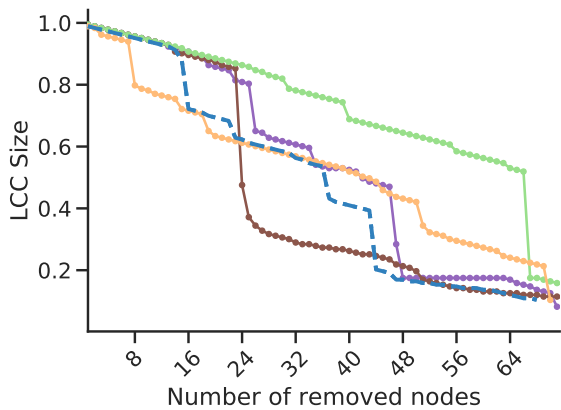
(f) hyves



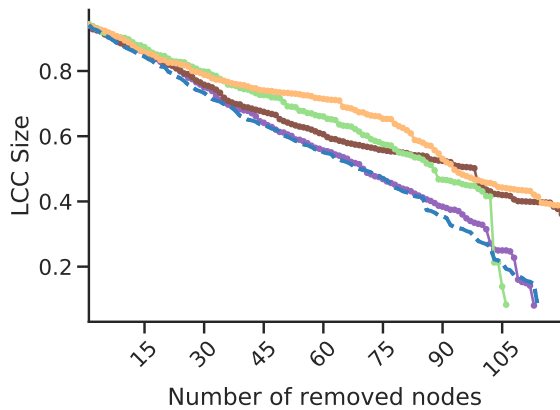
(g) inf-USAir97



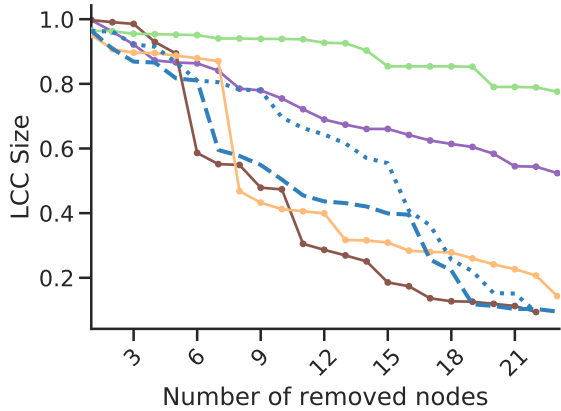
(h) librec-ciaodvd-trust



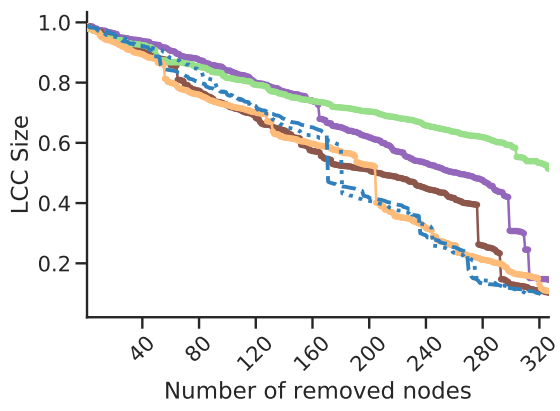
(i) maayan-foodweb



(j) maayan-Stelzl



(k) moreno-crime-projected



(l) opsahl-openflights

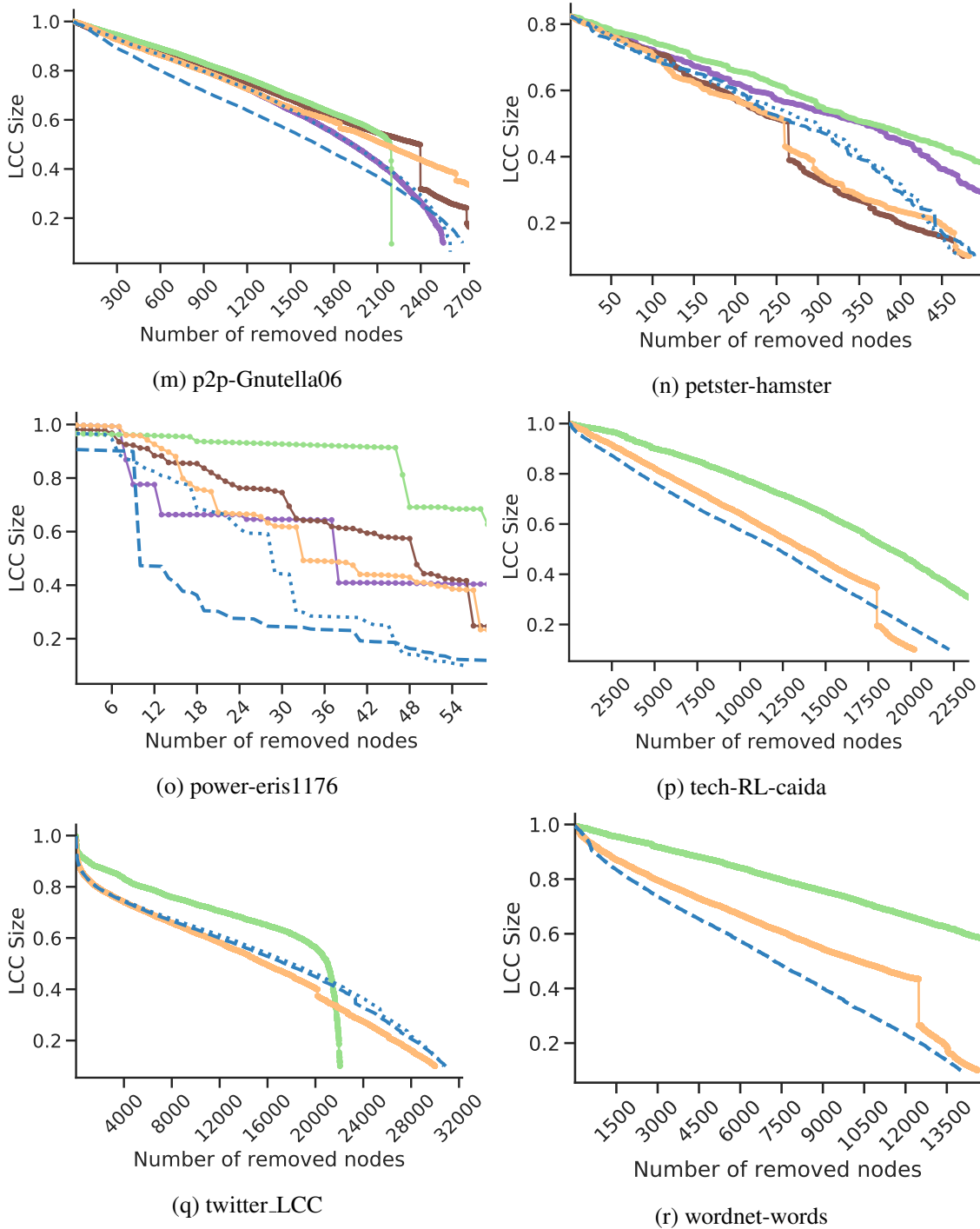
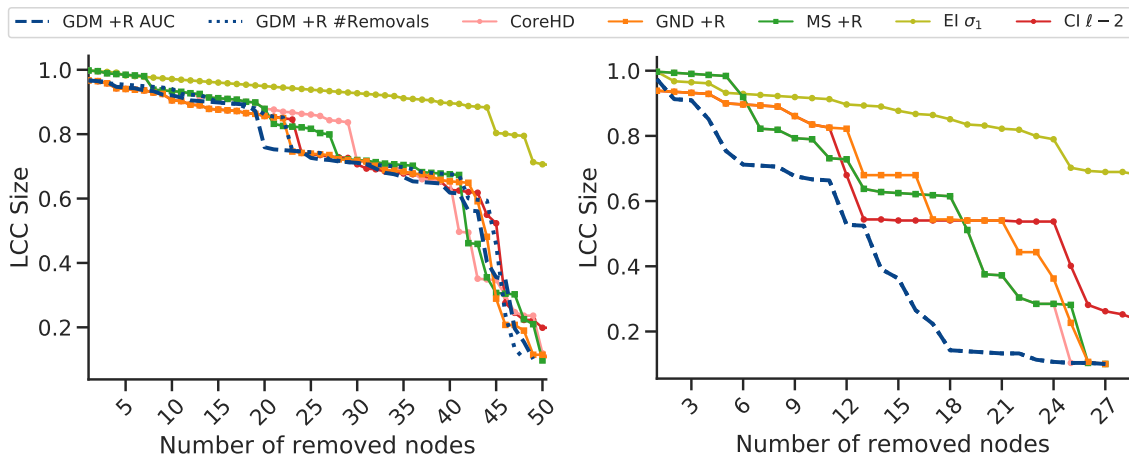
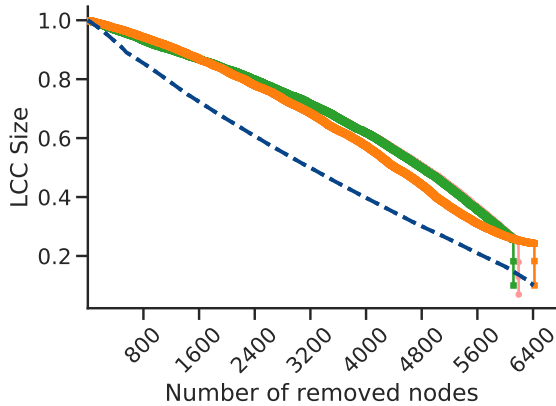


Figure 6: Dismantling of some networks in our test set. We compare against the algorithms without reinsertion in Tables 1 and 2 and show both the models with lower area under the curve (GDM AUC) and with lower number of removals (GDM #Removals), which may overlap for some networks.

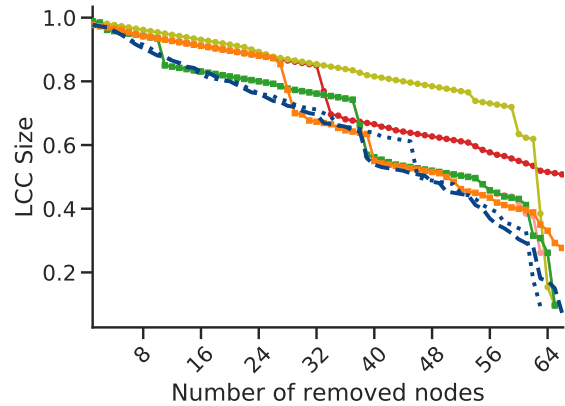


(a) arenas-meta

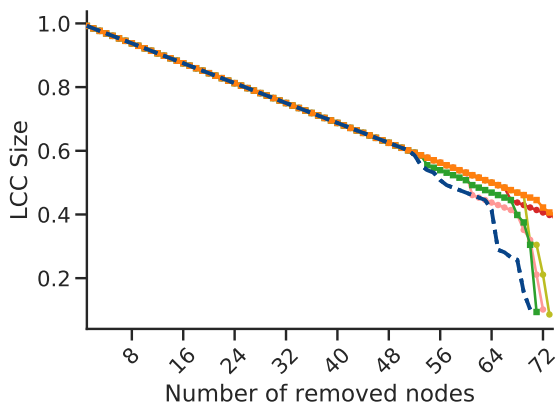
(b) corruption



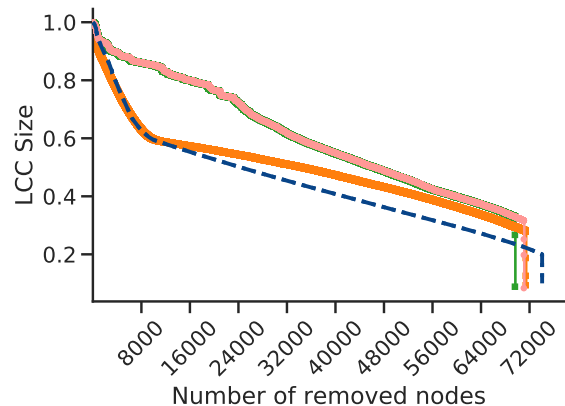
(c) douban



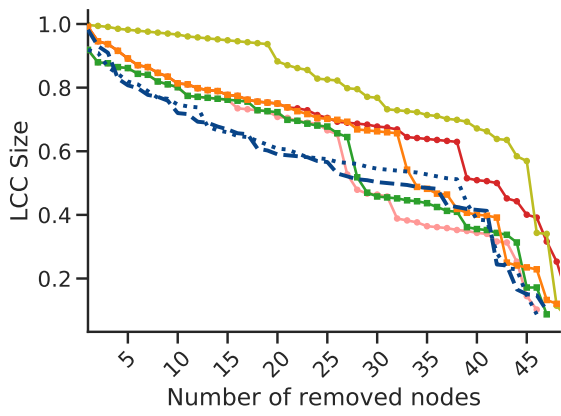
(d) econ-wm1



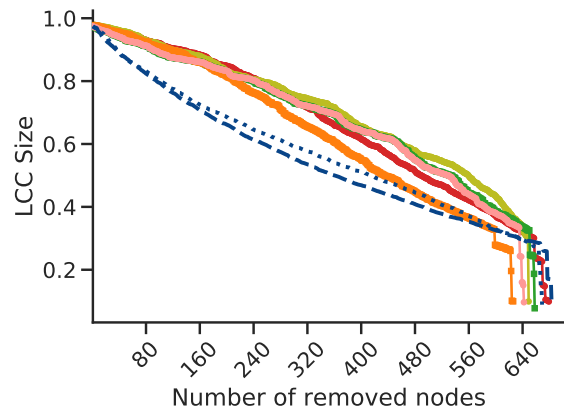
(e) foodweb-baywet



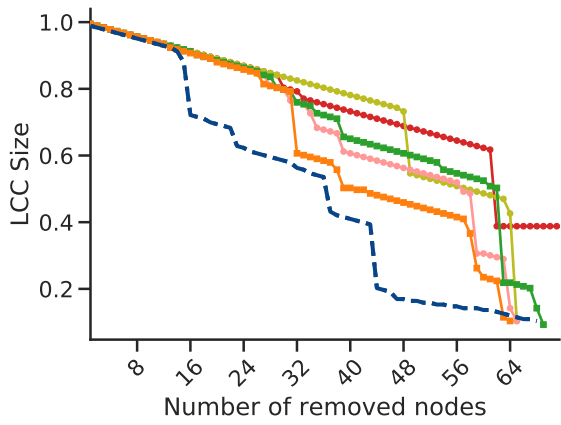
(f) hyves



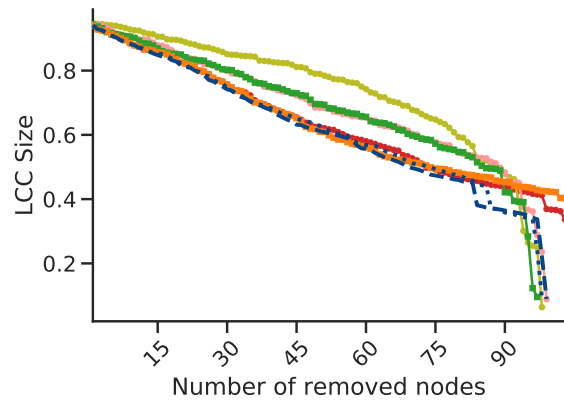
(g) inf-USAir97



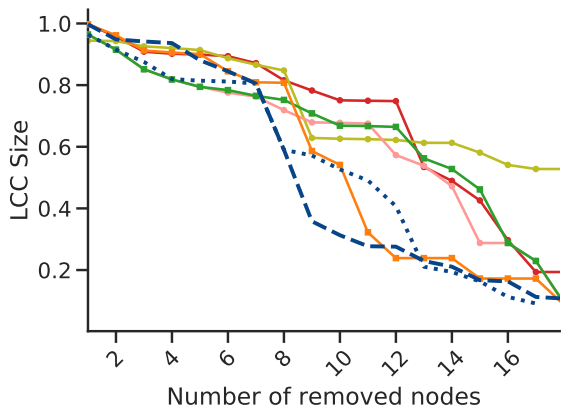
(h) librec-ciaodvd-trust



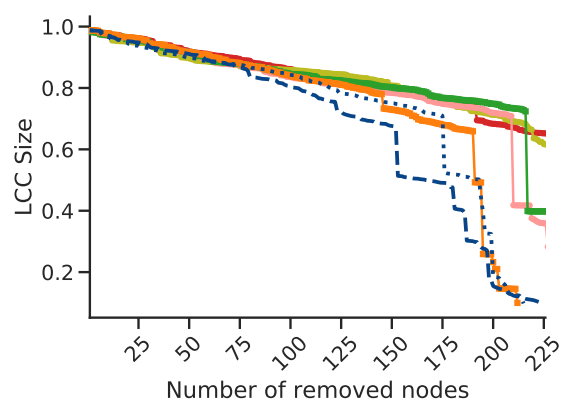
(i) maayan-foodweb



(j) maayan-Stelzl



(k) moreno-crime-projected



(l) opsahl-openflights

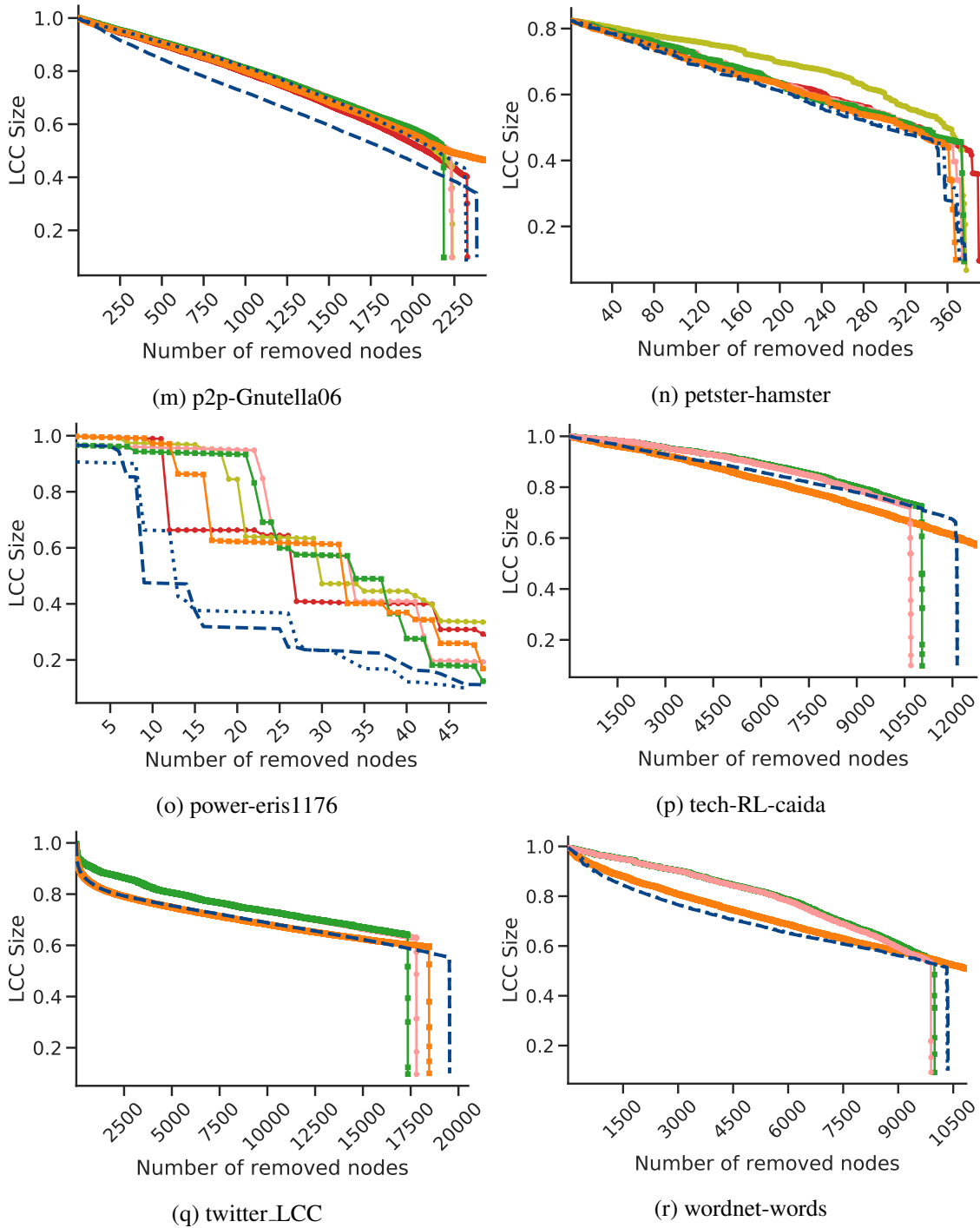


Figure 7: Dismantling of some networks in our test set. We compare against the algorithms with reinsertion phase in Tables 1 and 2 and show both the models with lower area under the curve (GDM +R AUC) and with lower number of removals (GDM +R #Removals), which may overlap for some networks.

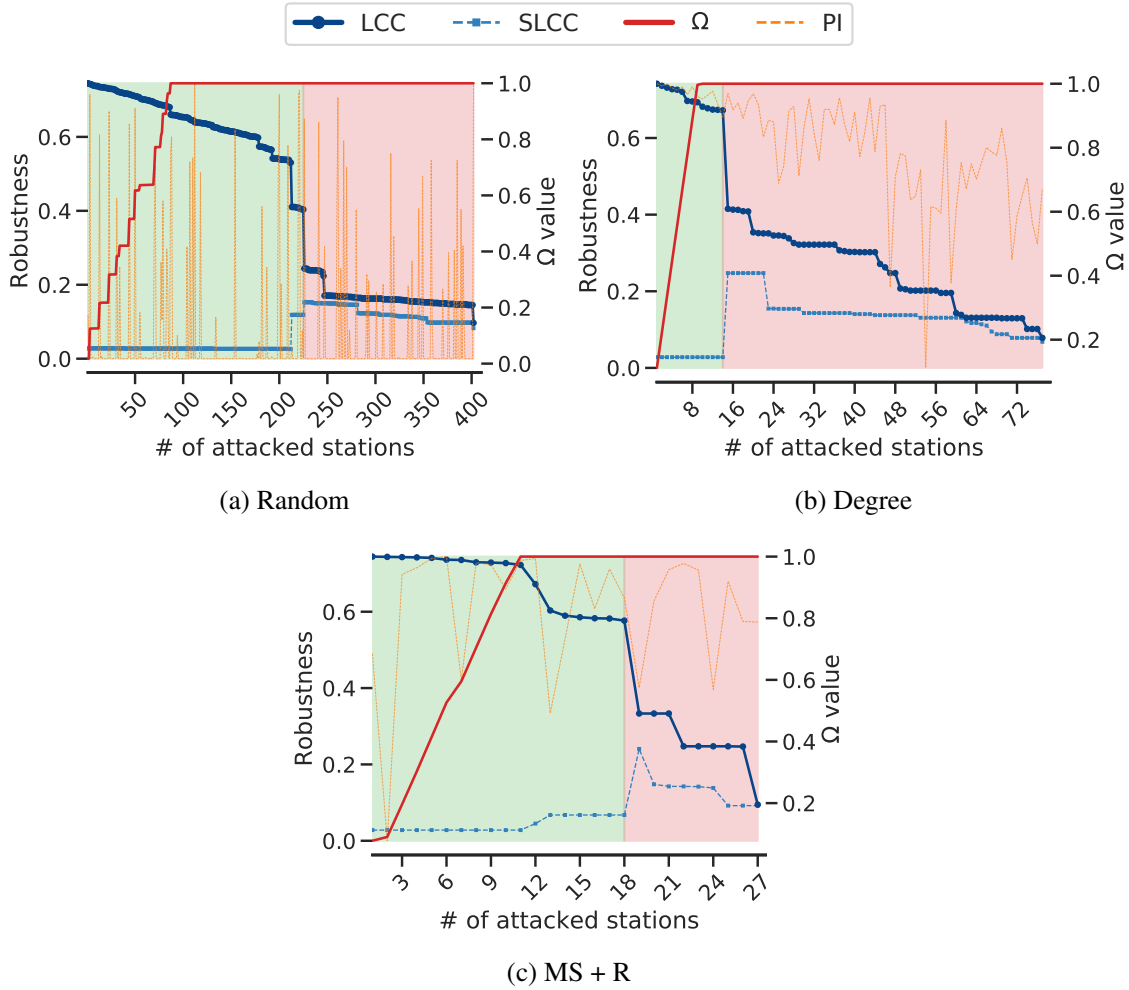


Figure 8: Early Warning values for the SciKit European powergrid under random failures and targeted attacks.

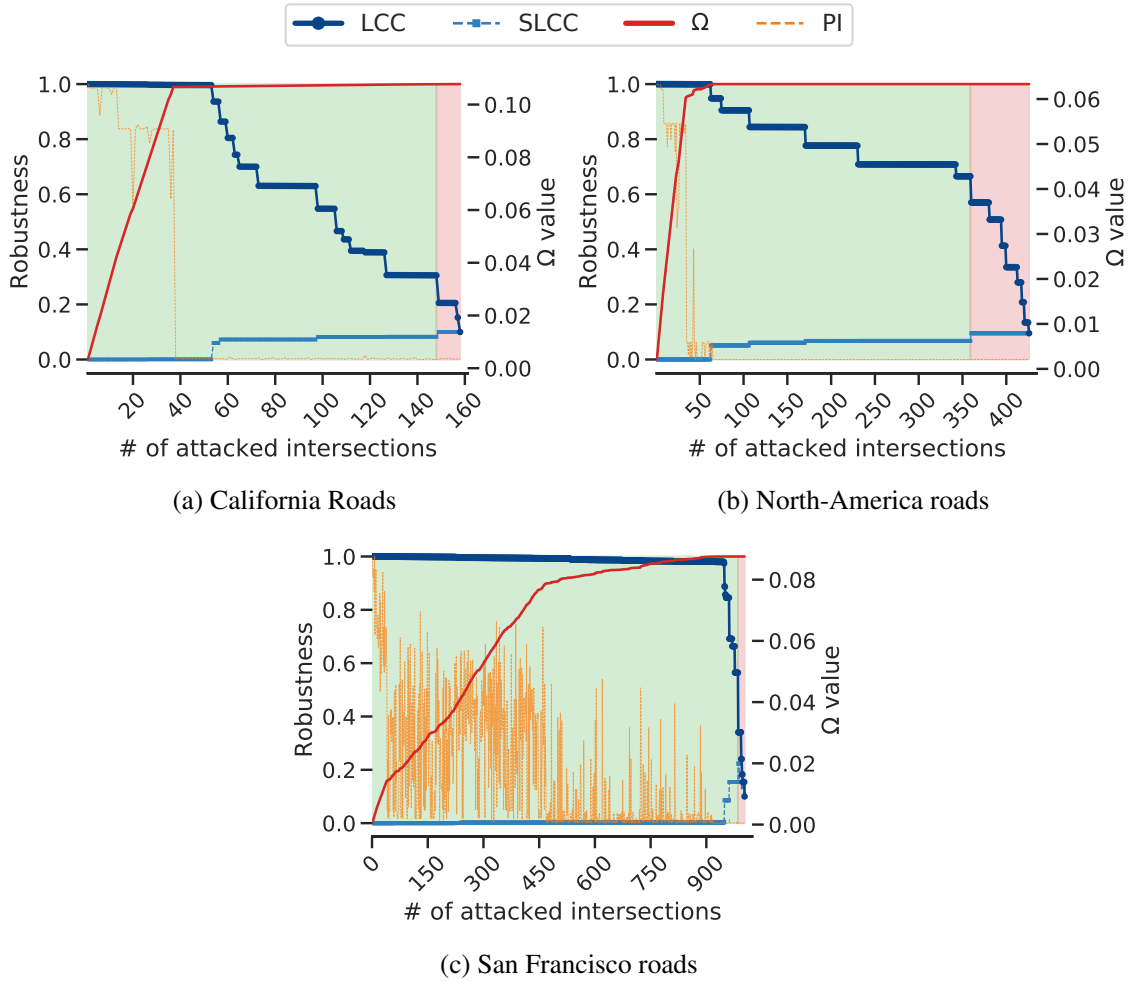


Figure 9: Ω values for three different American road networks under *GND* +R attacks (with cost matrix $\mathbf{W} = \mathbf{I}$).

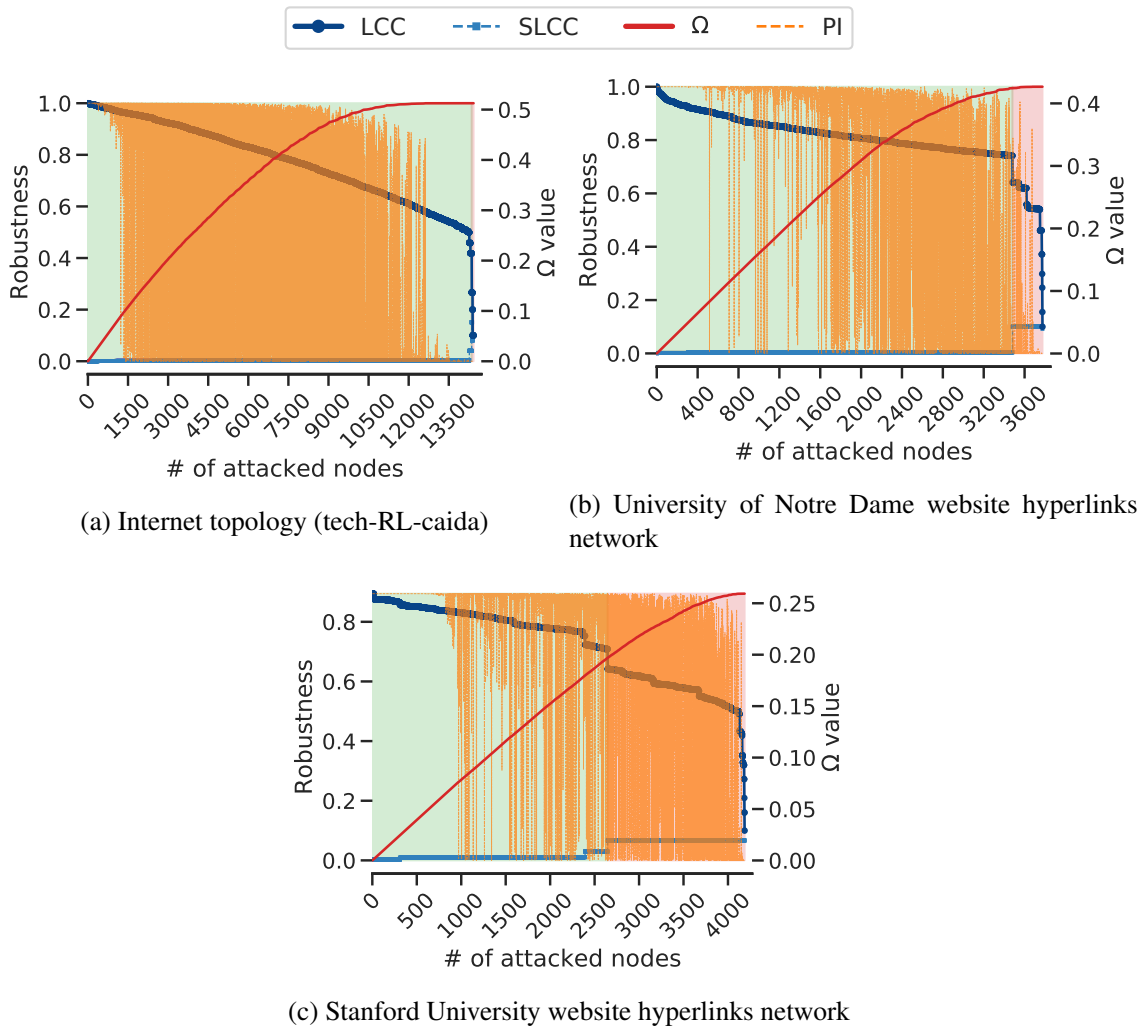


Figure 10: Ω values for three different internet networks under GND +R attacks (with cost matrix $\mathbf{W} = \mathbf{I}$).

Network	Name	Category	N	E	References
ARK201012_LCC	CAIDA ARK (Dec 2010) (LCC)	Infrastructure	29.3K	78.1K	(53)
advogato	Advogato trust network	Social	6.5K	43.3K	(2, 82)
arenas-meta	C. elegans	Metabolic	453	2.0K	(4, 60)
cfinder-google	Google.com internal	Hyperlink	15.8K	149.5K	(17, 89)
citeseer	CiteSeer	Citation	384.4K	1.7M	(6, 51)
com-dblp	DBLP co-authorship	Coauthorship	317.1K	1.0M	(8, 103)
corruption	Corruption Scandals	Social	309	3.3K	(92)
dblp-cite	DBLP citation	Citation	12.6K	49.6K	(9, 78)
digg-friends	Digg friends	Social	279.6K	1.5M	(10, 70)
dimacs10-celegansneural	C. elegans (neural)	Neural	297	2.1K	(41, 100, 101)
dimacs10-polblogs	Political blogs (LCC)	Hyperlink	1.2K	16.7K	(45, 48)
douban	Douban social network	Social	154.9K	327.2K	(12, 104)
econ-wm1	Economic network WM1	Economic	260	2.6K	(94)
ego-twitter	Twitter lists	Social	23.4K	32.8K	(37, 84)
email-EuAll	EU institution email	Communication	265.2K	365.6K	(13, 75)
eu-powergrid	SciGRID Power Europe	Power	1.5K	1.8K	(83)
foodweb-baydry	Florida ecosystem dry	Trophic	128	2.1K	(14, 98)
foodweb-baywet	Florida ecosystem wet	Trophic	128	2.1K	(15, 98)
gridkit-eupowergrid	GridKit Power Europe	Power	13.8K	17.3K	(102)
gridkit-north_america	GridKit Power North-America	Power	16.2K	20.2K	(102)
hyves	Hyves social network	Social	1.4M	2.8M	(23, 104)
inf-USAir97	US Air lines (1997)	Infrastructure	332	2.1K	(50, 94)
internet-topology	Internet (AS) topology	Infrastructure	34.8K	107.7K	(24, 105)
librec-ciaodvd-trust	CiaoDVD trust network	Social	4.7K	33.1K	(42, 65)
librec-filmtrust-trust	FilmTrust trust network	Social	874	1.3K	(44, 64)
linux	Linux source code files	Software	30.8K	213.7K	(26)
loc-brightkite	Brightkite friendships	Social	58.2K	214.1K	(3, 54)
loc-gowalla	Gowalla friendships	Social	196.6K	950.3K	(18, 54)
london_transport_multiplex_aggr	Aggregated London Transportation network	Transport	369	430	(59)
maayan-Stelzl	Human protein (Stelzl)	Metabolic	1.7K	3.2K	(21, 96)
maayan-figeys	Human protein (Figeys)	Metabolic	2.2K	6.4K	(20, 61)
maayan-foodweb	Little Rock Lake food web	Trophic	183	2.5K	(27, 81)
maayan-vidal	Human protein (Vidal)	Metabolic	3.1K	6.7K	(22, 95)
moreno_crime_projected	Crime (projection)	Social	754	2.1K	(7)
moreno_propro	Protein	Metabolic	1.9K	2.3K	(30, 57, 68, 97)
moreno_train	Train bombing terrorist contacts	Human contact	64	243	(35, 69)
munmun_digg_reply_LCC	Digg social network replies (LCC)	Communication	29.7K	84.8K	(11, 56)
munmun_twitter_social	Twitter follows (ICWSM)	Social	465.0K	833.5K	(36, 55)
opsahl-openflights	OpenFlights	Infrastructure	2.9K	15.7K	(29, 86)
opsahl-powergrid	US power grid	Infrastructure	4.9K	6.6K	(39, 100)
opsahl-ucsocial	UC Irvine messages	Communication	1.9K	13.8K	(38, 87)
oregon2_010526	Autonomous systems Oregon-2	Infrastructure	11.5K	32.7K	(74)
p2p-Gnutella06	Gnutella P2P, August 8 2002	Computer	8.7K	31.5K	(76, 93)
p2p-Gnutella31	Gnutella P2P, August 31 2002	Computer	62.6K	147.9K	(16, 93)
pajek-erdos	Erdős co-authorship network	Coauthorship	6.9K	11.8K	(43, 50)
petster-catdog-household	Catster/Dogster familylinks (LCC)	Social	324.9K	2.6M	(5)
petster-hamster	Hamsterster full	Social	2.4K	16.6K	(19)
power-eris1176	Power network problem	Power	1.2K	9.9K	(94)
roads-california	California Road Network	Infrastructure	21.0K	21.7K	(79)
roads-northamerica	North-America Road Network	Infrastructure	175.8K	179.1K	(80)
roads-sanfrancisco	San Francisco Road Network	Infrastructure	175.0K	221.8K	(52)
route-views	Autonomous systems AS-733	Infrastructure	6.5K	13.9K	(31, 75)
slashdot-threads	Slashdot threads	Communication	51.1K	117.4K	(32, 66)
slashdot-zoo	Slashdot Zoo	Social	79.1K	467.7K	(33, 73)
subelj_jdk	JDK dependency network	Software	6.4K	53.7K	(1)
subelj_jung-j	JUNG and Javax dependency network	Software	6.1K	50.3K	(25, 99)
tech-RL-caida	Internet router network	Infrastructure	190.9K	607.6K	(94)
twitter_LCC	Twitter users (LCC)	Social	532.3K	694.6K	(85)
web-EPA	Pages linking to epa.gov	Hyperlink	4.3K	8.9K	(94)
web-NotreDame	Notre Dame web pages	Hyperlink	325.7K	1.1M	(28, 49)
web-Stanford	Stanford University web pages	Hyperlink	281.9K	2M	(34, 77)
web-webbase-2001	Web network	Hyperlink	16.1K	25.6K	(94)
wikipedia_link_kn	Wikipedia links (KN)	Hyperlink	29.5K	278.7K	(47)
wikipedia_link_li	Wikipedia links (LI)	Hyperlink	49.1K	294.3K	(46)
wordnet-words	WordNet lexical network	Lexical	146.0K	657.0K	(40, 62)

Table 4: The networks used to evaluate our approach. For each network, we report the name, the number of nodes and edges, the category it belongs to and some references.